Documentos de Trabalho

Working Paper Series

"The Continuous Wavelet Transform: A Primer*"

Luís Aguiar-Conraria
Maria Joana Soares

NIPE WP 23/ 2010

NÚCLEO DE INVESTIGAÇÃO EM POLÍTICAS ECONÓMICAS
UNIVERSIDADE DO MINHO

"The Continuous Wavelet Transform: A Primer*"

Luís Aguiar-Conraria
Maria Joana Soares

NIPE* WP 23/ 2010

URL:
http://www.eeg.uminho.pt/economia/nipe

* NIPE – *Núcleo de Investigação em Políticas Económicas* – is supported by the Portuguese Foundation for Science and Technology through the *Programa Operacional Ciência, Teconologia e Inovação* (POCI 2010) of the *Quadro Comunitário de Apoio III*, which is financed by FEDER and Portuguese funds.

The Continuous Wavelet Transform: A Primer*

Luís Aguiar-Conraria† Maria Joana Soares‡

August 20, 2010

Abstract

Wavelet analysis is becoming more popular in the Economics discipline. Until recently, most works have made use of tools associated with the Discrete Wavelet Transform. However, after 2005, there has been a growing body of work in Economics and Finance that makes use of the Continuous Wavelet Transform tools. In this article, we give a self-contained summary on the most relevant theoretical results associated with the Continuous Wavelet Transform, the Cross-Wavelet Transform, the Wavelet Coherency and the Wavelet Phase-Difference. We describe how the transforms are usually implemented in practice and provide some examples. We also introduce the Economists to a new class of analytic wavelets, the Generalized Morse Wavelets, which have some desirable properties and provide an alternative to the Morlet Wavelet. Finally, we provide a user friendly toolbox which will allow any researcher to replicate our results and to use it in his/her own research.

Keywords: Economic cycles; Continuous Wavelet Transform, Cross-Wavelet Transform, Wavelet Coherency, Wavelet Phase-Difference; The Great Moderation.

1 Introduction

Economic agents simultaneously operate at different horizons. For example, central banks have different objectives in the short and long run, and operate simultaneously at different frequencies (see Ramsey and Lampart [39]). More than that, many economic processes are the result of the actions of several agents, who have different term objectives. Therefore, economic time-series are a combination of components operating on different frequencies. Several questions about the data are connected to the understanding of the time-series behavior at different frequencies.

*There is a Matlab toolbox associated with this paper, called ASToolbox, which is available at http://sites.google.com/site/aguiarconraria/joanasoares-wavelets.

†NIPE and Economics Department, University of Minho. E-mail: lfaguiar@eeg.uminho.pt

‡Department of Mathematics and Applications, University of Minho. E-mail: jsoares@math.uminho.pt

Fourier analysis allows us to study the cyclical nature of a time-series in the frequency domain. In spite of its utility, however, under the Fourier transform, the time information of a time series is completely lost. Because of this loss of information it is hard to distinguish transient relations or to identify when structural changes do occur. Moreover, these techniques are only appropriate for time-series with stable statistical properties, i.e. stationary time-series.

As an alternative, wavelet analysis has been proposed. Wavelet analysis performs the estimation of the spectral characteristics of a time-series as a function of time revealing how the different periodic components of the time-series change over time. One major advantage afforded by the wavelet transform is the ability to perform natural local analysis of a time series. It stretches into a long wavelet function to measure the low frequency movements; and it compresses into a short wavelet function to measure the high frequency movements.

Wavelets are becoming part of the standard set of tools available to an economist. The pioneering work of Ramsey and Lampart [39, 38] and Ramsey [36, 37] was followed by Gençay, Selçuk and B. Withcher [21, 20, 22], Wong, Ip, Xie and Lui [45], Connor and Rossiter [9], Fernandez [15] and Gallegati and Gallegati [17]. However, all these works have one common characteristic. They all rely on the Discrete Wavelet Transform (DWT).[1]

More recently, tools associated with the Continuous Wavelet Transform are becoming more widely used. Raihan, Wen and Zeng [35], Jagrič and Ovin [27], Crowley and Mayes [10], Aguiar-Conraria, Azevedo and Soares [1], Baubeau and Cazelles [3], Rua and Nunes [41], Rua [40] and Aguiar-Conraria and Soares [2]; provide some examples of useful economic applications of these tools.

Unfortunately, in our opinion, there is no good single reference for someone wanting to use (continuous) wavelet tools, such as: the Continuous Wavelet Transform, the Cross-Wavelet Transform, the Wavelet Coherency and the Wavelet Phase-Difference. Not only the theoretic foundations are scattered among several papers and books, but also most codes freely available imply rigid assumptions, which do not give much freedom of choice to the researcher. For example, all the works cited in the previous paragraph make use of the Morlet Wavelet.

This paper has three main purposes: (1) to give a self-contained summary on the most relevant theoretical results, (2) to describe how the transforms are usually implemented in practice and (3) to introduce the economist to a new family of wavelets that have some desirable characteristics and that have the potential to become as popular as the Morlet Wavelet. Attached to this paper, there is a Matlab toolbox implementing the referred wavelet tools, which the researcher can freely use and adapt to his/her own research.

Among the several examples that we analyse we consider two real data applications. In one of them, we show evidence that corroborates the arguments of Blanchard and Simon [5] about the Great Moderation, who have argued that the Great Moderation started well before 1983. In our second application we show how business cycles synchronization between two neighbor countries, Portugal and Spain, evolve and how they are affected but by changes

[1]For an excellent review on discrete wavelet applications in economics, see Crowley [11].

in their political and policy regimes.

This paper proceeds as follows. In Section 2, we describe the Continuous Wavelet Transform. In Section 3, we introduce the cross-wavelet tools, which include the Cross-Wavelet Power, Wavelet Coherency and Phase-Difference. Section 4 describes how to adapt the theory in order to implement it computationally. Section 5 summarizes some of the results already obtained in terms of significance testing. In Section 6, we describe some of the characteristics of the Morlet Wavelet, responsible for its popularity. We also introduce a new class of analytic wavelets, the Generalized Morse Wavelets (GMWs), that can potentially become as useful as the Morlet Wavelet. We show that while the Morlet wavelets represent a good compromise between frequency and time localization, GMWs allow for more flexibility. In section 7, we provide some constructed examples of wavelet applications and the two applications with real data. Section 8 concludes. In the appendix, we describe the ASToolbox and some of our computational choices.

2 Continuous Wavelet Transform

2.1 Notations and Conventions

In what follows, $L^2(\mathbb{R})$ denotes the set of square integrable functions, i.e. the set of functions defined on the real line and satisfying

$$\int_{-\infty}^{\infty} |x(t)|^2 \, dt < \infty, \tag{1}$$

with the usual inner product

$$\langle x, y \rangle := \int_{-\infty}^{\infty} x(t) y^*(t) dt \tag{2}$$

and associated norm

$$\|x\| := \langle x, x \rangle^{\frac{1}{2}}. \tag{3}$$

Here, and in what follows, the asterisk superscript is used to denote complex conjugation.

Since the (squared) norm of $x(t)$, $\|x(t)\|^2 = \int_{-\infty}^{\infty} |x(t)|^2 dt$ is usually referred to as the *energy* of x, the space $L^2(\mathbb{R})$ is also known as the space of finite energy functions.

In these notes, we always use the convention $g(t) \leftrightarrow G(\omega)$ to denote a Fourier pair, i.e. we denote by the the corresponding capital letter the Fourier transform of a given function. Hence, if $x(t) \in L^2(\mathbb{R})$, $X(\omega)$ will denote its Fourier transform, here defined as:

$$X(\omega) := \int_{-\infty}^{\infty} x(t) e^{-i\omega t} dt. \tag{4}$$

Note 2.1. With the above convention of the Fourier transform, ω is an *angular* (or radian) frequency. The relation to the more common Fourier frequency f is given by $f = \frac{\omega}{2\pi}$.

We recall the well-known Parseval relation, valid for all $x(t), y(t) \in L^2(\mathbb{R})$:

$$\langle x(t), y(t)\rangle = \frac{1}{2\pi}\langle X(\omega), Y(\omega)\rangle, \tag{5}$$

from which the Plancherel identity immediately follows:

$$\|x(t)\|^2 = \frac{1}{2\pi}\|X(\omega)\|^2. \tag{6}$$

2.2 Wavelets

The minimum requirement imposed on a function $\psi(t) \in L^2(\mathbb{R})$ to qualify for being a *mother* (*admissible* or *analyzing*) *wavelet* is that it satisfies a technical condition, usually referred to as the *admissibility condition*, which reads as follows:

$$0 < C_\psi := \int_{-\infty}^{\infty} \frac{|\Psi(\omega)|}{|\omega|} d\omega < \infty; \tag{7}$$

see [12, p.22]. The constant C_ψ above is called the *admissibility constant*.

The wavelet ψ is usually normalized to have unit energy: $\|\psi\|^2 = \int_{-\infty}^{\infty} |\psi(t)|^2\, dt = 1$.

We should point out that the square integrability of $\psi(t)$ is a very mild decay condition and that, in practice, much more stringent conditions are imposed. In fact, for the purpose of providing a useful time-frequency localization, the wavelet must be a reasonable well localized function, both in the time domain as well as in the frequency domain. For functions with sufficient decay, it turns out that the admissibility condition (7) is equivalent to requiring that

$$\Psi(0) = \int_{-\infty}^{\infty} \psi(t) dt = 0; \tag{8}$$

again, see Daubechies [12, p.24]. This means that the function ψ has to wiggle up and down the $t-$axis, i.e. it must behave like a wave; this, together with the assumed decaying property, justifies the choice of the term wavelet (originally, in French, *ondelette*) to designate ψ.

2.3 CWT

Starting with a mother wavelet ψ, a family $\psi_{\tau,s}$ of "wavelet daughters" can be obtained by simply scaling and translating ψ:

$$\psi_{\tau,s}(t) := \frac{1}{\sqrt{|s|}}\psi\left(\frac{t-\tau}{s}\right), \quad s, \tau \in \mathbb{R},\ s \neq 0, \tag{9}$$

where s is a scaling or dilation factor that controls the width of the wavelet (the factor $1/\sqrt{|s|}$ being introduced to guarantee preservation of the energy, $\|\psi_{\tau,s}\| = |\psi|$) and τ is a translation parameter controlling the location of the wavelet. Scaling a wavelet simply

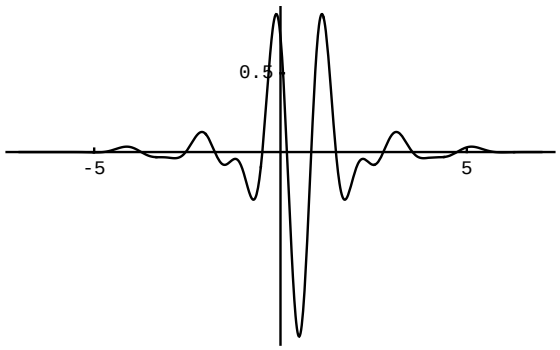

Figure 1: A typical wavelet

means stretching it (if $|s| > 1$) or compressing it (if $|s| < 1$), while translating it simply means shifting its position in time.

Given a time-series $x(t) \in L^2(\mathbb{R})$, its *Continuous Wavelet Transform* (CWT) with respect to the wavelet ψ is a function of two variables, $W_{x;\psi}(\tau, s)$, obtained by projecting $x(t)$, in the L^2 sense, onto the family $\{\psi_{\tau,s}\}$:

$$W_{x;\psi}(\tau, s) = \langle x, \psi_{\tau,s} \rangle = \int_{-\infty}^{\infty} x(t) \frac{1}{\sqrt{|s|}} \psi^* \left(\frac{t-\tau}{s} \right) dt. \tag{10}$$

Note 2.2. When the wavelet ψ is implicit from the context, we abbreviate the notation and simply write W_x for $W_{x;\psi}$.

By well-known properties of the Fourier transform, one immediately sees that the CWT (10) may also be represented in the frequency, as

$$W_x(\tau, s) = \frac{\sqrt{|s|}}{2\pi} \int_{-\infty}^{\infty} \Psi^*(s\omega) X(\omega) e^{i\omega\tau} d\omega. \tag{11}$$

2.4 Inversion of CWT

The importance of the admissibility condition (7) comes from the fact that its fulfilment guarantees that the energy of the original function $x(t)$ is preserved by the wavelet transform, i.e., the following Parseval-type relation holds:

$$\int_{-\infty}^{\infty} |x(t)|^2 dt = \frac{1}{C_\psi} \int_{-\infty}^{\infty} \int_{-\infty}^{\infty} |W_x(\tau, s)|^2 \frac{d\tau ds}{s^2}, \tag{12}$$

which, in turn, ensures the possibility of recovering $x(t)$ from its wavelet transform. In fact, due to the high redundancy of this transform (recall that a function of one variable is

mapped into a bivariate function), many reconstruction formulas are available. For example, when the wavelet ψ is real-valued, it is possible to reconstruct $x(t)$ by using the formula

$$x(t) = \frac{2}{C_\psi} \int_0^\infty \left[\int_{-\infty}^\infty W_x(\tau, s) \psi_{\tau,s}(t) d\tau \right] \frac{ds}{s^2}, \tag{13}$$

showing that no information is lost if we restrict the computation of the transform only to positive values of the scaling parameter s, which is a usual requirement, in practice.

One can also limit the integration over a selected range of scales, performing a band-pass filtering of the original series.

2.5 Wavelet Power Spectrum and Wavelet Phase

In analogy with the terminology used in the Fourier case, the (local) *Wavelet Power Spectrum* (sometimes called *Scalogram* or *Wavelet Periodogram*) is defined as

$$(WPS)_x(\tau, s) = |W_x(\tau, s)|^2 . \tag{14}$$

The Wavelet Power Spectrum may be averaged over time for comparison with classical spectral methods. When the average is taken over all times, we obtain the so-called *Global Wavelet Power Spectrum*:

$$(GWPS)_x(s) = \int_{-\infty}^\infty |W_x(\tau, s)|^2 \, d\tau. \tag{15}$$

When the wavelet ψ is complex-valued, the corresponding wavelet transform $W_x(\tau, s)$ is also complex-valued. In this case, the transform can be separated into its real part, $\Re\{W_x(\tau, s)\}$, and imaginary part, $\Im\{W_x(\tau, s)\}$, or in its *amplitude*, $|W_x(\tau, s)|$, and *phase* (or phase-angle), $\phi_x(\tau, s) : W_x(\tau, s) = |W_x(\tau, s)| \, e^{i\phi_x(\tau,s)}$. Recall that the phase-angle $\phi_x(\tau, s)$ of the complex number $W_x(\tau, s)$ can be obtained from the formula:

$$\phi_x(\tau, s) = \text{Arctan}\big(\frac{\Im\{W_x(\tau, s)\}}{\Re\{W_x(\tau, s)\}}\big). \tag{16}$$

Note 2.3. We use Arctan to denote the following extension of the usual principal component of the arctan function (whose range is $(-\pi/2, \pi/2)$):

$$\text{Arctan}\left(\frac{b}{a}\right) = \begin{cases} \arctan(\frac{b}{a}) & a > 0, \\ \arctan(\frac{b}{a}) + \pi & a < 0, \quad b \geq 0, \\ \arctan(\frac{b}{a}) - \pi & a < 0, \quad b < 0, \\ \pi/2 & a = 0, \quad b \geq 0, \\ -\pi/2 & a = 0, \quad b < 0. \end{cases}$$

For real-valued wavelet functions, the imaginary part is constantly zero and the phase is, therefore, undefined. Hence, in order to separate the phase and amplitude information of a time-series, it is important to make use of complex wavelets. In this case, it is

convenient to choose a wavelet $\psi(t)$ whose Fourier transform is supported on the positive real-axis only, i.e. is such that $\Psi(\omega) = 0$ for $\omega < 0$. A wavelet satisfying this property is called *analytic* or *progressive*. When ψ is analytic and $x(t)$ is real, reconstruction formulas involving only positive values of the scale parameter s are still available; in particular, if the wavelet satisfies $0 < |K_\psi| < \infty$, where $K_\psi := \int_0^\infty \frac{\Psi^*(\omega)}{\omega} d\omega$, then one can use the following reconstruction formula, known as the *Morlet formula*, which is particularly useful for numerical applications:

$$x(t) = 2\Re\left[\frac{1}{K_\psi}\int_0^\infty W_x(t,s)\frac{ds}{s^{3/2}}\right]; \tag{17}$$

see, e.g. Farge [14] or Holschneider [25].

When the wavelet ψ is analytic, the corresponding wavelet transform is called an *Analytic Wavelet Transform* (AWT).

Remark: *Throughout the rest of this paper, we assume that all the wavelets considered are analytic and hence, that the wavelet transform is computed only for positive values of the scaling parameter s. For this reason, in all the formulas that would normally involve the quantity $|s|$, this will be replaced by s.*

2.6 Localization Properties

In order to describe the time-frequency localization properties of the CWT, we have to assume that both the wavelet $\psi(t)$ and its Fourier transform $\Psi(\omega)$ are well localized functions. More precisely, these functions must have sufficient decay to guarantee that the quantities defined below are all finite.[2] We define the *center in time* of the wavelet ψ , $\mu_{t;\psi}$, by

$$\mu_{t;\psi} = \frac{1}{\|\psi\|^2}\int_{-\infty}^{\infty} t\,|\psi(t)|^2\,dt, \tag{18}$$

and, as a measure of concentration of ψ around its center, we take the *standard deviation in time*, $\sigma_{t;\psi}$ (also known as the *radius in time*):

$$\sigma_{t;\psi} = \frac{1}{\|\psi\|}\left\{\int_{-\infty}^{\infty}(t-\mu_{t;\psi})^2\,|\psi(t)|^2\,dt\right\}^{\frac{1}{2}}. \tag{19}$$

The *center in frequency*, $\mu_{\omega;\psi}$, and the *standard deviation (or radius) in frequency*, $\sigma_{\omega;\psi}$, of ψ are defined as

$$\mu_{\omega;\psi} = \frac{1}{\|\Psi\|^2}\int_{-\infty}^{\infty}\omega\,|\Psi(\omega)|^2\,d\omega \tag{20}$$

and

$$\sigma_{\omega;\psi} = \frac{1}{\|\Psi\|}\left\{\int_{-\infty}^{\infty}(\omega-\mu_{\omega;\psi})^2\,|\Psi(\omega)|^2\,d\omega\right\}^{\frac{1}{2}}. \tag{21}$$

[2]The precise requirements are that $|\psi(t)| < C(1+|t|)^{-(1+\epsilon)}$ and $|\Psi(\omega)| < C(1+|\omega|)^{-(1+\epsilon)}$, for $C < \infty$, $\epsilon > 0$.

Note 2.4. 1. If wavelet ψ is known from the context, we will suppress the index ψ in the notation of the above quantities, e.g. we will simply use μ_t for $\mu_{t;\psi}$, etc.

2. The quantities μ_t and σ_t are the mean and standard deviation of the probability density function (p.d.f.) defined by $\frac{|\psi(t)|^2}{\|\psi\|^2}$; a similar meaning, but associated with the p.d.f. defined by $\frac{|\Psi(\omega)|^2}{\|\Psi\|^2}$, exists for μ_ω and σ_ω.

The interval $[\mu_t - \sigma_t, \mu_t + \sigma_t]$ is the set where $\psi(t)$ attains its "most significant" values whilst the interval $[\mu_\omega - \sigma_\omega, \mu_\omega + \sigma_\omega]$ plays the same role for $\Psi(\omega)$.

The rectangle

$$H_\psi := [\mu_t - \sigma_t, \mu_t + \sigma_t] \times [\mu_\omega - \sigma_\omega, \mu_\omega + \sigma_\omega] \tag{22}$$

in the (t, ω) −plane is called the *Heisenberg box* or *window* for the function ψ. We then say that ψ is localized around the point (μ_t, μ_ω) of the time-frequency plane, with *uncertainty* given by A_ψ, where

$$A_\psi := \sigma_t \sigma_\omega. \tag{23}$$

The value A_ψ is also called the *Heisenberg area* associated with the function ψ and is conventionally used as a measure of the degree of energy localization of the wavelet.[3] The Heisenberg uncertainty principle establishes that the Heisenberg area is bounded from below by the quantity 1/2, i.e. for all $\psi \in L^2(\mathbb{R})$, we have

$$\sigma_t \sigma_\omega \geq \frac{1}{2}. \tag{24}$$

Recalling that the wavelet daughter $\psi_{\tau,s}$ is obtained from its mother ψ by a simple translation by τ and a scaling by s, it is very easy to show that the center and radius in time of $\psi_{\tau,s}$ are given by $\mu_{t;\psi_{\tau,s}} = \tau + s\mu_t$ and $\sigma_{t;\psi_{\tau,s}} = s\sigma_t$. Also, from well-known properties of the Fourier transform, one can easily show that the center and radius in frequency of $\psi_{\tau,s}$ are given by $\mu_{\omega;\psi_{\tau,s}} = \frac{\mu_\omega}{s}$ and $\sigma_{\omega;\psi_{\tau,s}} = \frac{\sigma_\omega}{s}$, respectively. In particular, if the mother wavelet ψ is centered at $t = 0$, i.e. if $\mu_t = 0$,[4] then the window associated with $\psi_{\tau,s}$ becomes

$$H_{\psi_{\tau,s}} = [\tau - s\sigma_t, \tau + s\sigma_t] \times \left[\frac{\mu_\omega}{s} - \frac{\sigma_\omega}{s}, \frac{\mu_\omega}{s} + \frac{\sigma_\omega}{s}\right]. \tag{25}$$

In this case, one has

$$W_x(\tau, s) = \langle x(t), \psi_{\tau,s}(t) \rangle = \int_{-\infty}^{\infty} x(t)\psi^*_{\tau,s}(t)dt \approx \int_{\tau - s\sigma_t}^{\tau + s\sigma_t} x(t)\psi^*_{\tau,s}(t)dt \tag{26}$$

and, by the Parseval relation,

$$W_x(\tau, s) = 2\pi \langle X(\omega), \Psi_{\tau,s}(\omega) \rangle = 2\pi \int_{-\infty}^{\infty} X(\omega)\Psi^*_{\tau,s}(\omega)d\omega \approx 2\pi \int_{\frac{\mu_\omega}{s} - \frac{\sigma_\omega}{s}}^{\frac{\mu_\omega}{s} + \frac{\sigma_\omega}{s}} X(\omega)\Psi_{s,\tau}(\omega)d\omega. \tag{27}$$

---

[3] This value is simply $\frac{1}{4}$ of the area of the Heisenberg window H_ψ, which justifies the name.

[4] Note that this can easily be achieved by an appropriate translation.

We thus conclude that the continuous wavelet transform $W_x(\tau, s)$ gives us temporal information on $x(t)$ around the instant $t(\tau) = \tau$, with precision $s\sigma_t$, and frequency information about $X(\omega)$ around the frequency

$$\omega(s) = \frac{\mu_\omega}{s}, \tag{28}$$

with precision $\frac{\sigma_\omega}{s}$.

Although the area of the windows is constant (given by $4\sigma_t\sigma_\omega$), their dimensions change according to the scale; the windows stretch for large values of s (broad scales s – low frequencies $\omega_s = \frac{\sigma_\omega}{s}$) and compress for small values of s (fine scale – high frequencies $\frac{\sigma_\omega}{s}$). This is one major advantage afforded by the wavelet transform, when compared, with the other standard method of time-frequency localization, the *short time Fourier transform*: its ability to perform natural local analysis of a time-series in the sense that the length of wavelets varies endogenously; it stretches into a long wavelet function to measure the low frequency movements; and it compresses into a short wavelet function to measure the high frequency movements.

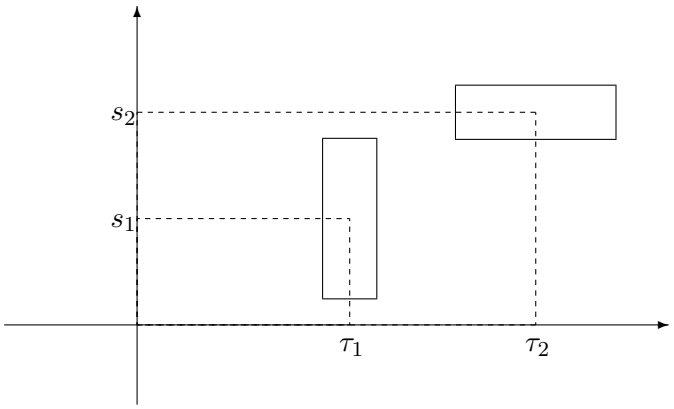

Figure 2: Windows associated with a wavelet transform

2.7 Scale/Frequency Relation and Fourier Factor

Formula (20) is commonly used to convert scales into frequencies. But, we should have in mind that this inverse relation between scale and frequency corresponds to a particular interpretation and that there are other meaningful ways of assigning frequencies to scales. In Lilly and Olhede[31], the authors consider, apart from value of $\mu_{\omega;\psi}$ given by (20), which they call the *energy-frequency*, and which, for convenience, we will now denote by ω_ψ^E, i.e.

$$\omega_\psi^E = \frac{1}{\|\Psi\|^2} \int_{-\infty}^{\infty} \omega \, |\Psi(\omega)|^2 \, d\omega, \tag{29}$$

two other specific frequencies associated with the wavelet:

- the *peak frequency*, ω_ψ^P, defined as the frequency at which the magnitude of the Fourier transform of ψ, $|\Psi(\omega)|$, is maximized, i.e.

$$|\Psi(\omega_\psi^P)| = \sup_{\omega\in\mathbb{R}} |\Psi(\omega)|; \tag{30}$$

- the *central instantaneous frequency*, ω_ψ^I, defined as the value that the so-called *time-varying instantaneous frequency* of the wavelet takes at its center (here assumed to be 0), i.e.

$$\omega_\psi^I = \breve{\omega}_\psi(0), \tag{31}$$

  where $\breve{\omega}(t)$, is the time-varying instantaneous frequency of the wavelet, defined by

$$\breve{\omega}_\psi(t) = \frac{d}{dt}\Im\{\ln\psi(t)\} = \frac{d}{dt}\arg\{\psi(t)\}. \tag{32}$$

To each of the three specific frequencies, $\omega_\psi^E, \omega_\psi^P$ and ω_ψ^I they associate an interpretation of scale as frequency. More precisely, they define

$$\omega(s) = \frac{\omega_\psi}{s}, \tag{33}$$

with ω_ψ denoting any of the three specific frequencies. Note that $\omega(s)$, as well as $\omega_\psi^E, \omega_\psi^P$ and ω_ψ^I, are all angular frequencies. If we prefer a relation between the scale and the usual "Fourier" frequency f (expressed in cycles per unit time), we have

$$f(s) = \frac{\omega_\psi}{2\pi s}. \tag{34}$$

The relation between scale and wavelength or period (inverse of usual frequency) is, therefore, given by

$$\lambda(s) = \frac{2\pi}{\omega_\psi}s. \tag{35}$$

The factor

$$\mathrm{Ff} := \frac{2\pi}{\omega_\psi} \tag{36}$$

is referred to as the *Fourier factor* of the wavelet and is used, in the programs, to convert scales to periods.

To see that the three correspondences $\omega(s) = \frac{\omega_\psi}{s}$, $\omega_\psi = \omega_\psi^P, \omega_\psi^E, \omega_\psi^I$ are all meaningful (although in different senses) we refer the reader to the mentioned paper by Lilly and Olhede [31].

Naturally, it will be convenient to choose a wavelet whose associated frequencies $\omega_\psi^E, \omega_\psi^P$ and ω_ψ^I have all the same (or, at least, very similar) value, since this will give us a unified view of the relation between frequency and scale.

3 Cross-Wavelet Analysis

In many applications, one is interested in detecting and quantifying relationships between two non-stationary time series. The concepts of Cross-Wavelet Power, Wavelet Coherency and Wavelet Phase-Difference are natural generalizations of the basic wavelet analysis tools that enable us to appropriately deal with the time-frequency dependencies between two time-series.

Remark: *From now on, all the quantities we are going to introduce (e.g. Cross-Wavelet Transform, Wavelet Coherency, etc.) are functions of time and scale (or frequency). In order to simplify the notation, we will describe these quantities for a specific value of the argument* (τ, s) *and this value of the argument will, unless strictly necessary, be omitted in the formulas.*

3.1 Cross-Wavelet Transform and Cross-Wavelet Power

The *Cross-Wavelet Transform* (XWT) of two time-series, $x(t)$ and $y(t)$, first introduced by Hudgins, Friehe and Mayer [26], is simply defined as

$$W_{xy} = W_x W_y^*, \tag{37}$$

where W_x and W_y are the wavelet transforms of x and y, respectively. [5]

We also define the *Cross-Wavelet Power*, as

$$(XWP)_{xy} = |W_{xy}| . \tag{38}$$

While we can interpret the Wavelet Power Spectrum as depicting the local variance of a time-series, the Cross-Wavelet Power of two time-series depicts the local covariance between these time-series at each time and frequency. Therefore, the Cross-Wavelet Power gives us a quantified indication of the similarity of power between two time-series.

3.2 Complex Wavelet Coherency

In analogy with the concept of coherency used in Fourier analysis, given two time-series $x(t)$ and $y(t)$ one can define their *Complex Wavelet Coherency* ϱ_{xy} by:

$$\varrho_{xy} = \frac{\mathscr{S}(W_{xy})}{\left[\mathscr{S}(|W_x|^2)\,\mathscr{S}(|W_y|^2)\right]^{1/2}}, \tag{39}$$

where $\mathscr{S}$ denotes a smoothing operator in both time and scale; smoothing is necessary, because, otherwise, coherency would be identically one at all scales and times. Time and scale smoothing can be achieved, e.g. by convolution with appropriate windows; see Cazelles, Chavez, de Magny, Guégan and Hales [7] or Grinsted, Moore and Jevrejeva [24], for details.

[5] When $y = x$, we obtain the Wavelet Power Spectrum $W_{xx} = |W_x|^2 = (WPS)_x$.

3.3 Wavelet Coherency and Phase-Lead

The complex wavelet coherency can be written in polar form, as $\varrho_{xy} = |\varrho_{xy}|\, e^{i\phi_{xy}}$. The absolute value of the complex wavelet coherency is called the *Wavelet Coherency* and is denoted by R_{xy}, i.e.

$$R_{xy} = \frac{|\mathscr{S}(W_{xy})|}{\left[\mathscr{S}(|W_x|^2)\,\mathscr{S}(|W_y|^2)\right]^{1/2}}. \tag{40}$$

The angle ϕ_{xy} of the complex coherency is called the *Phase-Difference* (phase lead of x over y), i.e.

$$\phi_{xy} = \mathrm{Arctan}\Big(\frac{\Im(\mathscr{S}(W_{xy}))}{\Re(\mathscr{S}(W_{xy}))}\Big) \tag{41}$$

Note 3.1.

1. As in the case of the usual (Fourier) coherency, Wavelet Coherency satisfies the inequality
$$0 \le R_{xy}(\tau, s) \le 1 \tag{42}$$
whenever the ratio (40) is well defined. At points (τ, s) for which
$$\mathscr{S}\left(|W_x(\tau, s)|^2\right)\mathscr{S}\left(|W_y(\tau, s)|^2\right) = 0$$
we will define $R_{xy}(\tau, s) = 0$.

2. The Phase-Difference is sometimes defined using the spectra without smoothing, i.e.
$$\phi_{xy} = \mathrm{Arctan}\Big(\frac{\Im(W_{xy})}{\Re(W_{xy})}\Big). \tag{43}$$
In this case, one has $\phi_{xy} = \phi_x - \phi_y$, [6] justifying its name.

A Phase-Difference of zero indicates that the time series move together at the specified time-frequency; if $\phi_{xy} \in (0, \frac{\pi}{2})$, then the series move in phase, but the time-series y leads x; if $\phi_{xy} \in (-\frac{\pi}{2}, 0)$, then it is x that is leading; a Phase-Difference of π (or $-\pi$) indicates an anti-phase relation; if $\phi_{xy} \in (\frac{\pi}{2}, \pi)$, then x is leading; time-series y is leading if $\phi_{xy} \in (-\pi, -\frac{\pi}{2})$.

With the Phase-Difference, one can also calculate the *Instantaneous Time-Lag* between the two time-series x and y:

$$(\Delta T)_{xy}(\tau, s) = \frac{\phi_{xy}(\tau, s)}{\omega(\tau)}, \tag{44}$$

where $\omega(\tau)$ is the angular frequency that corresponds to the scale s.

[6] To be more precise, the above relation holds after we convert $\phi_x - \phi_y$ into an angle in the interval $[-\pi, \pi]$.

4 Discrete Computations

4.1 Discretized CWT

Suppose we sample the series $x(t)$ with a fine enough sample interval δt to avoid aliasing (i.e. assume that $X(\omega) \approx 0$ for $|\omega| > \frac{2\pi}{2\delta t} = \frac{\pi}{\delta t}$) and use the shorthand notation $x_n = x(n\delta t); n = 0, \ldots, N-1$. Also, let $\boldsymbol{x} = \{x_n; n = 0, \ldots, N-1\}$. With N even, formula (11) can be discretized as

$$\begin{aligned} W_x(\tau, s) &\approx \frac{\sqrt{s}}{2\pi} \int_{-\frac{\pi}{\delta t}}^{\frac{\pi}{\delta t}} X(\omega) \Psi^*(s\omega)\, e^{i\omega\tau} d\omega \\ &\approx \frac{\sqrt{s}}{2\pi} \frac{2\pi}{N\delta t} \sum_{k=-(N/2)+1}^{N/2} X\left(\frac{2\pi k}{N\delta t}\right) \Psi^*\left(\frac{s2\pi k}{N\delta t}\right) e^{i\frac{2\pi k}{N\delta t}\tau} \\ &= \frac{\sqrt{s}}{N\delta t} \sum_{k=-(N/2)+1}^{N/2} X\left(\frac{2\pi k}{N\delta t}\right) \Psi^*\left(\frac{s2\pi k}{N\delta t}\right) e^{i\frac{2\pi k}{N\delta t}\tau} \end{aligned}$$

But, $X\left(\frac{2\pi k}{N\delta t}\right) \approx \delta t\, \hat{x}_k$, where $\hat{x}_k = \sum_{n=0}^{N-1} x_n e^{-i2\pi nk/N}$ is the kth element of the Discrete Fourier Transform (DFT) of the N-vector $(x_0, \ldots, x_{N-1})$; see e.g. Brémaud [6, p.99]. Hence, we obtain a discretized form of the CWT of the discrete time-series $\boldsymbol{x} = \{x_n : 0, \ldots, N-1\}$:

$$\begin{aligned} W_{\boldsymbol{x}}(\tau, s) &= \frac{\sqrt{s}}{N} \sum_{k=0}^{N/2} \hat{x}_k \Psi^*(s\frac{2\pi k}{N\delta t}) e^{\frac{i2\pi k\tau}{N\delta t}} \\ &\quad + \frac{\sqrt{s}}{N} \sum_{k=(N/2)+1}^{N-1} \hat{x}_k \Psi^*(s\frac{2\pi(k-N)}{N\delta t}) e^{\frac{i2\pi(k-N)\tau}{N\delta t}} \end{aligned}$$

where we used the periodicity $\hat{x}_k = \hat{x}_{k-N}$. When $\tau = m\,\delta t;\ m = 0, \ldots, N-1$, we get

$$\begin{aligned} W_{\boldsymbol{x}}(m\delta t, s) &= \frac{\sqrt{s}}{N} \sum_{k=0}^{N/2} \hat{x}_k \Psi^*(s\frac{2\pi k}{N\delta t}) e^{\frac{i2\pi km}{N}} \\ &\quad + \frac{\sqrt{s}}{N} \sum_{k=(N/2)+1}^{N-1} \hat{x}_k \Psi^*(s\frac{2\pi(k-N)}{N\delta t}) e^{\frac{i2\pi km}{N}} \\ &= \frac{\sqrt{s}}{N} \sum_{k=0}^{N-1} \hat{x}_k \Psi^*(s w_k) e^{\frac{i2\pi km}{N}} \end{aligned}$$

where

$$w_k = \begin{cases} \frac{2\pi k}{N\delta t}, & k = 0, 1, \ldots, \frac{N}{2}, \\ \frac{2\pi(k-N)}{N\delta t}, & k = \frac{N}{2}+1, \ldots, N-1. \end{cases} \tag{45}$$

In practice, naturally, the wavelet transform is computed only for a selected set of scale values $s \in \{s_\ell, \ell = 0, \ldots, F-1\}$ (corresponding to a certain choice of frequencies ω_ℓ). Hence, our computed wavelet spectrum of the discrete-time series $\boldsymbol{x}$ will simply be a $F \times N$ matrix $\mathbf{W}_{\boldsymbol{x}}$ (wavelet spectral matrix) whose (ℓ, m) element is given by

$$\mathbf{W}_{\boldsymbol{x}}(\ell, m) = \frac{\sqrt{s_\ell}}{N} \sum_{k=0}^{N-1} \hat{x}_k \Psi^*(s_\ell w_k) e^{\frac{i2\pi km}{N}}, \tag{46}$$

with w_k given by (45).[7] The above formula is an efficient formula for computing the CWT, since, for each scale s_ℓ, its right-hand side is simply the inverse DFT of the sequence $(z_0^\ell, \ldots, z_{N-1}^\ell)$ where

$$z_k^\ell := \sqrt{s_\ell}\, \hat{x}_k\, \Psi^*(s_\ell\, w_k); k = 0, \ldots, N-1,$$

and can, therefore, be calculated using an inverse FFT.

4.1.1 Choice of scales

The scales are usually chosen as fractional powers of 2:

$$s_\ell = s_0\, 2^{\frac{\ell}{n_V}}; \ell = 0, 1, \ldots, n_V \times n_O, \tag{47}$$

where n_O denotes the number of octaves (i.e. powers of two) and n_V the number of voices calculated per octave (i.e., $F = n_V \times n_O + 1$).

4.1.2 Cone of influence

As with other types of transforms, the CWT applied to a finite length time-series inevitably suffers from border distortions; this is due to the fact that the values of the transform at the beginning and the end of the time-series are always incorrectly computed, in the sense that they involve missing values of the series which are then artificially prescribed. When using the formula (46), a periodization of the data is assumed. However, before implementing formula (46), one usually pads the series with zeros, to avoid wrapping. Since the "effective support" of the wavelet at scale s is proportional to s, these edge-effects also increase with s. The region in which the transform suffers from these edge effects is called the cone of influence (COI). In this area of the time-frequency plane the results are subject to border distortions and have to be interpreted carefully.

[7] We choose to make the row indexes of the matrix correspond to scales and the columns to times, so that the plots of this matrix will naturally lead to times in the x-axis and frequencies (or periods) in the y-axis.

4.2 Other Discretized Wavelet Measures

Naturally, all the formulas given previously for other wavelet measures, such as the Cross-Wavelet Transform, the Wavelet Coherency and the Phase-Difference have discrete counterparts. For example, corresponding to formula (37) for the Cross-Wavelet Transform, we have a discretized version

$$\mathbf{W}_{\boldsymbol{xy}}(\ell, m) = \mathbf{W}_{\boldsymbol{x}}(\ell, m)\mathbf{W}^{*}_{\boldsymbol{y}}(\ell, m). \tag{48}$$

Formula (43) for the phase-difference is discretized as

$$\phi_{\boldsymbol{xy}}(\ell, m) = \text{Arctan}\big(\frac{\Im\left(\mathbf{W}_{\boldsymbol{xy}}(\ell, m)\right)}{\Re\left(\mathbf{W}_{\boldsymbol{xy}}(\ell, m)\right)}\big). \tag{49}$$

5 Significance Tests

As with other time-series methods, it is important to assess the statistical significance of the results obtained by wavelet analysis.

The seminal paper by Torrence and Compo [43] is one of the first works to discuss significance testing for wavelet and cross-wavelet power.

By using a large number of Monte Carlo simulations, Torrence and Compo concluded that the local wavelet power spectrum of a white or red noise signal, normalized by the signal variance, has a chi-squared distribution:

$$D\left(\frac{\left|W_x\left(s,\tau\right)\right|^2}{\sigma_x^2} < p\right) = \frac{1}{2}P_f\chi^2_v.$$

In the expression above, the value P_f is the mean spectrum of the background noise at the Fourier frequency f that corresponds to the wavelet scale s and ν is equal to 1 or 2, for real or complex wavelets, respectively.

Torrence and Compo also derived empirical distributions for Cross-Wavelet Power. If two time-series are generated by stationary processes with Fourier spectra P^x_k and P^y_k then the cross wavelet distribution is given by

$$D\left(\frac{|W_{xy}(\tau, s)|}{\sigma_x\sigma_y} < p\right) = \frac{Z_\nu(p)}{\nu}\sqrt{P^x_k P^y_k},$$

where, again, ν is 1 for real wavelets and 2 for complex wavelets and $Z_\nu(p)$ is the confidence level for a given probability p for the square root of two chi-squared distributions; one can find the confidence level Z_ν by inverting the integral $p = \int_0^{Z_\nu} f_\nu(z)dz$,where the p.d.f is given by

$$f_\nu(z) = \frac{2^{2-\nu}}{\Gamma^2(\nu/2)}z^{\nu-1}K_0(z),$$

where z is the random variable , Γ is the Gamma function $\Gamma(z) := \int_0^\infty t^{z-1}e^{-t}dt$ and $K_0(z)$ is the modified Bessel function of order zero.

Two recent paper by Z. Ge,[18] and [19], reconsider the discussion of the significance testing for the wavelet and cross-wavelet power.

In the first paper, the authors concentrate on the use of a specific wavelet (a Morlet Wavelet) and, assuming a Gaussian white noise process, analytically derive the corresponding sampling distribution of the Wavelet Power. The results obtained are in agreement with the numerical conclusions from Torrence and Compo; however, this sampling distribution was shown to be highly dependent on the local covariance structure of the wavelet, a fact that makes the significance levels intimately related to the specific wavelet family used, contradicting a statement made in Torrence and Compo [43].

In the second paper, the authors also derive analytical distributions for the Cross-Wavelet Power Spectrum and Wavelet Coherence. Here, again, the analysis is done only for the case of the Morlet Wavelet and with the assumption of two independent Gaussian white noise background processes. For more general processes, one has to rely on Monte-Carlo simulations.

6 Analytic Wavelets

The admissibility condition (7) is a very weak condition and, in theory, there are infinitely many wavelets.

In practice, the choice of which wavelet to use is an important aspect to be taken into account, and will be dictated by the kind of application one has in mind.

To study the synchronism between different time-series, it is important to select a wavelet whose corresponding transform contains information on both amplitude and phase, and hence, a complex-valued analytic wavelet is a natural choice.

As stated in Lilly and Olhede [31], the analytic wavelet transform (AWT) is the basis for the *wavelet ridge* method, Delprat, Escudié, Guillemain, Kronland-Martinet, Tchamitchian and and B. Torrésani [13], Mallat [32], which recovers time-varying estimates of instantaneous amplitude, phase, and frequency of a modulated oscillatory signal from the time/scale plane. On the other hand, the analytic wavelet transform can also be useful for application to very time-localized structures Tu, Hwang and Ho [44]. The many useful features of analytic wavelets are covered in more depth by Selesnick, Baraniuk and Kinsbury [42]; see also Olhede and Walden [34] and Lilly and Olhede [31].

In this section, we summarize some results concerned with the most used wavelet in practice, the Morlet Wavelet (to our knowledge, every application of the continuous wavelet transform in Economics have used this choice). We also present a particularly important family of analytic wavelets, the so-called Generalized Morse Wavelets (GMWs), which are more flexible and can be used as an alternative to the Morlet Wavelet. The results of this section are derived from the papers by Olhede and Walden [34] and Lilly and Olhede [30, 31].

6.1 Morlet Wavelets

The *Morlet Wavelets* are a one-parameter family of functions, first introduced in Goupillaud, Grossman and Morlet [23], and given by

$$\psi_{\omega_0}(t) = Ke^{i\omega_0 t}e^{-\frac{t^2}{2}}. \tag{50}$$

Strictly speaking, the above functions are not true wavelets, since they fail to satisfy the admissibility condition. [8] For $\psi_{\omega_0}(t)$ to have unit energy, the normalizing constant K must be chosen as

$$K = \pi^{-1/4}, \tag{51}$$

which, from now on, we will always assume to be true. The Fourier transform of the normalized wavelet is given by

$$\Psi_{\omega_0}(\omega) = \sqrt{2}\pi^{1/4}\, e^{-\frac{1}{2}(\omega-\omega_0)^2} \tag{52}$$

and, hence, $\Psi_{\omega_0}(0) = \sqrt{2}\pi^{1/4}\, e^{-{\omega_0}^2/2} \neq 0$. However, for sufficiently large ω_0, e.g. $\omega_0 > 5$, the values of $\Psi\omega_0(\omega)$ for $\omega \leq 0$ are so small that, for numerical purposes, Ψ_{ω_0} can be considered as an analytic wavelet; see Foufoula-Georgiou and Kumar [16].

The Morlet Wavelet became the most popular of the complex valued wavelets mainly because of four interesting properties. First, for numerical purposes, as we have just seen, it can be treated as an analytic wavelet. Second, the peak frequency, the energy frequency and the central instantaneous frequency of the Morlet Wavelet are all equal and given by

$$\omega^P_{\psi_{\omega_0}} = \omega^E_{\psi_{\omega_0}} = \omega^I_{\psi_{\omega_0}} = \omega_0, \tag{53}$$

facilitating the conversion from scales to frequencies. Third, the Heisenberg box area reaches its lower bound with this wavelet, i,e, the uncertainty attains the minimum possible value: $\sigma_{t;\psi_{\omega_0}}\sigma_{\omega;\psi_{\omega_0}} = \frac{1}{2}$. In this sense, the Morlet Wavelet has optimal joint time-frequency concentration. Finally, the time radius and the frequency radius are equal,

$$\sigma_{t;\psi\omega_0} = \sigma_{\omega;\psi\omega_0} = \frac{1}{\sqrt{2}}, \tag{54}$$

and, therefore, this wavelet represents the best compromise between time and frequency concentration.

6.2 Generalized Morse Wavelets

In spite of its usefulness, the Morlet Wavelet suffers from some limitations. Mainly, because it depends on just one parameter, implying that it is not very versatile. On top of that,

[8] In order to fulfill the admissibility condition, a correction term has to be added, as: $\psi_{\omega_0}(t) = K\left(e^{i\omega_0 t} - e^{-\omega_0^2/2}\right)e^{-t^2/2}$.

because, even for numerical purposes, it cannot be considered analytic for $\omega_0 < 5$, the parameter choices are very restricted. To our knowledge, at least in economics, every paper uses some value of $\omega_0 \in [5, 6]$. Finally, although it is true that the Morlet Wavelet has optimal joint time-frequency concentration in the Heisenberg sense, it is also true that there are other criteria available. "The whole set of generalized Morse wavelets are optimally localized in that they maximize the eigenvalues of a joint time-frequency localization operator (...) and indeed this is the way the generalized Morse wavelets were initially constructed." – in Lilly and Olhede [31, p.150].

The generalized Morse wavelets (GMWs) are a two-parameter family of wavelets, defined, in the frequency domain, by

$$\Psi_{\beta,\gamma}(\omega) = K_{\beta,\gamma}\, H(\omega)\, \omega^{\beta} e^{-\omega^{\gamma}} \tag{55}$$

where $K_{\beta,\gamma}$ is a normalizing constant and $H(\omega)$ is the Heaviside unit step function.

To be a valid wavelet, one must have $\beta > 0$ and $\gamma > 0$. By varying these two parameters, the generalized Morse wavelets can be given a broad range of characteristics while remaining exactly analytic. In fact, these wavelets form a very wide family that subsumes may other types of wavelets. It was shown in Lilly and Olhede [31] that the generalized Morse wavelets encompass two other popular families of analytic wavelets: the Cauchy or Klauder wavelet family (for $\gamma = 1$)[9] and the analytic "Derivative of Gaussian" wavelets (for $\gamma = 2$).

The normalizing constant is frequently taken to ensure that the value of the Fourier transform of the wavelet at the peak frequency is equal to 2, i.e. $\Psi(\omega_{\psi}^{P}) = 2$. In order for this to happen, the constant must be chosen as

$$K_{\beta,\gamma} = K_{\beta;\gamma}^{P} := 2\left(\frac{e\,\gamma}{\beta}\right)^{\beta/\gamma} \tag{56}$$

see, e.g. Lilly and Olhede [31, p.147].

Sometimes, the constant $K_{\beta,\gamma}$ is chosen in order to guarantee that $\psi_{\beta,\gamma}(t)$ has unit energy, i.e. $\|\psi_{\beta,\gamma}\|^2 = \int_{-\infty}^{\infty} |\psi_{\beta,\gamma}(t)|^2 dt = 1$, which, by the Parseval's identity, is equivalent to requiring that $\|\Psi_{\beta,\gamma}\|^2 = \int_{0}^{\infty} |\Psi_{\beta,\gamma}(\omega)|^2 d\omega = 2\pi$.[10] The corresponding value of the constant is given by

$$K_{\beta;\gamma} = K_{\beta,\gamma}^{E} := \frac{2^{(r+1)/2}\sqrt{\pi\gamma}}{\sqrt{\Gamma(r)}} \tag{57}$$

where

$$r = \frac{2\beta + 1}{\gamma} \tag{58}$$

and Γ is the gamma function; see, e.g. Olhede and Walden [34, p. 2663].

[9] The Paul wavelets correspond to the case $\gamma = 1$ and $\beta \in \mathbb{N}$

[10] The last integral extends only from 0 to ∞ due to the analyticity of the wavelet.

6.2.1 Measures for the GMWs

Remark: *When using a generalized Morse wavelet $\psi_{\beta,\gamma}$ with parameters β and γ, the subscript "ψ" of any quantity referring to the wavelet ψ will be replaced by "β, γ"; e.g., the energy frequency ω_{ψ}^{E} of $\psi_{\beta,\gamma}$ will be denoted by $\omega_{\beta,\gamma}^{E}$, etc.*

For the generalized Morse wavelets, we have:

- The peak frequency is given by

$$\omega_{\beta,\gamma}^{P} = \left(\frac{\beta}{\gamma}\right)^{1/\gamma}. \tag{59}$$

- The energy frequency is given by

$$\omega_{\beta,\gamma}^{E} = \frac{1}{2^{1/\gamma}} \frac{\Gamma(\frac{2\beta+2}{\gamma})}{\Gamma(\frac{2\beta+1}{\gamma})}. \tag{60}$$

- The central instantaneous frequency is given by

$$\omega_{\beta,\gamma}^{I} = \frac{\Gamma(\frac{\beta+2}{\gamma})}{\Gamma(\frac{\beta+1}{\gamma})} = 2^{1/\gamma}\omega_{\beta/2,\gamma}^{E}. \tag{61}$$

- The (squared) radius in time is given by

$$\sigma_{t;\beta,\gamma}^{2} = \frac{1}{\tilde{\Gamma}\left(\frac{2\beta+1}{\gamma}\right)} \left\{ \beta^2 \tilde{\Gamma}\left(\frac{2\beta-1}{\gamma}\right) + \gamma^2 \tilde{\Gamma}\left(\frac{2\beta+2\gamma-1}{\gamma}\right) - 2\beta\gamma\tilde{\Gamma}\left(\frac{2\beta+\gamma-1}{\gamma}\right) \right\}, \tag{62}$$

  where we have introduced the notation

$$\tilde{\Gamma}(z) := \frac{\Gamma(z)}{2^z};$$

  the above formula can be derived in a similar manner to Formula (47) in Lilly and Olhede [31].

- The frequency-domain radius (squared) is given by

$$\sigma_{\omega;\beta,\gamma}^{2} = \frac{1}{2^{2/\gamma}} \left\{ \frac{\Gamma\left(\frac{2\beta+3}{\gamma}\right)}{\Gamma\left(\frac{2\beta+1}{\gamma}\right)} - \left(\frac{\Gamma\left(\frac{2\beta+2}{\gamma}\right)}{\Gamma\left(\frac{2\beta+1}{\gamma}\right)} \right)^2 \right\}; \tag{63}$$

  the above formula can be derived in a similar manner to Formula (45) in Lilly and Olhede [31].

A table with the localization measures (time-radius, frequency-radius and Heisenberg area) for GMW $\psi_{\beta;\gamma}$, for the values $\beta, \gamma = 1, \ldots, 10$, is given below. In the last row, we also indicate the measures for the Morlet Wavelet.

Table 1: Measures for GMW

β	γ	σ_t	σ_ω	Heis. Area	β	γ	σ_t	σ_ω	Heis. Area
1	1	1.0000	0.8660	0.8660	6	1	0.3015	1.8028	0.5436
	2	1.7321	0.3367	0.5832		2	1.4460	0.3500	0.5061
	3	2.0622	0.2576	0.5312		3	2.4178	0.2069	0.5002
	4	2.2870	0.2283	0.5222		4	3.1682	0.1584	0.5019
	5	2.4701	0.2138	0.5281		5	3.7732	0.1343	0.5067
	6	2.6314	0.2055	0.5406		6	4.2827	0.1198	0.5130
	7	2.7788	0.2003	0.5564		7	4.7262	0.1101	0.5202
	8	2.9162	0.1968	0.5740		8	5.1219	0.1031	0.5280
	9	3.0460	0.1945	0.5923		9	5.4815	0.0978	0.5362
	10	3.1695	0.1928	0.6111		10	5.8129	0.0937	0.5448
2	1	0.5774	1.1180	0.6455	7	1	0.2774	1.9365	0.5371
	2	1.5275	0.3438	0.5252		2	1.4412	0.3505	0.5051
	3	2.0967	0.2405	0.5043		3	2.4749	0.2021	0.5002
	4	2.4928	0.2025	0.5048		4	3.2864	0.1527	0.5017
	5	2.8036	0.1831	0.5133		5	3.9450	0.1282	0.5059
	6	3.0655	0.1715	0.5256		6	4.5011	0.1136	0.5115
	7	3.2960	0.1638	0.5400		7	4.9857	0.1039	0.5178
	8	3.5045	0.1585	0.5555		8	5.4180	0.0968	0.5247
	9	3.6968	0.1546	0.5716		9	5.8107	0.0915	0.5319
	10	3.8763	0.1517	0.5880		10	6.1723	0.0874	0.5394
3	1	0.4472	1.3229	0.5916	8	1	0.2582	2.0616	0.5323
	2	1.4832	0.3468	0.5144		2	1.4376	0.3509	0.5044
	3	2.1941	0.2285	0.5014		3	2.5262	0.1980	0.5001
	4	2.7060	0.1859	0.5032		4	3.3931	0.1478	0.5016
	5	3.1091	0.1642	0.5106		5	4.1011	0.1232	0.5053
	6	3.4468	0.1511	0.5208		6	4.7005	0.1086	0.5103
	7	3.7415	0.1424	0.5326		7	5.2233	0.0988	0.5159
	8	4.0059	0.1361	0.5454		8	5.6898	0.0917	0.5220
	9	4.2477	0.1315	0.5587		9	6.1134	0.0864	0.5285
	10	4.4720	0.1280	0.5724		10	6.5034	0.0823	0.5352
4	1	0.3780	1.5000	0.5669	9	1	0.2425	2.1794	0.5286
	2	1.4639	0.3484	0.5099		2	1.4349	0.3512	0.5039
	3	2.2798	0.2196	0.5007		3	2.5729	0.1944	0.5001
	4	2.8839	0.1743	0.5026		4	3.4908	0.1436	0.5014
	5	3.3635	0.1513	0.5089		5	4.2446	0.1189	0.5048
	6	3.7654	0.1374	0.5174		6	4.8845	0.1043	0.5093
	7	4.1153	0.1281	0.5273		7	5.4431	0.0945	0.5144
	8	4.4281	0.1215	0.5379		8	5.9418	0.0875	0.5199
	9	4.7131	0.1165	0.5490		9	6.3947	0.0822	0.5257
	10	4.9766	0.1126	0.5605		10	6.8113	0.0781	0.5317
5	1	0.3333	1.6583	0.5528	10	1	0.2294	2.2913	0.5257
	2	1.4530	0.3493	0.5076		2	1.4327	0.3514	0.5034

(cont.)

Measures for GMW *(continued)*

β	γ	σ_t	σ_ω	Heis. Area	β	γ	σ_t	σ_ω	Heis. Area
	3	2.3535	0.2126	0.5004		3	2.6157	0.1912	0.5001
	4	3.0357	0.1654	0.5022		4	3.5810	0.1400	0.5013
	5	3.5815	0.1417	0.5076		5	4.3778	0.1152	0.5044
	6	4.0400	0.1275	0.5149		6	5.0557	0.1006	0.5085
	7	4.4389	0.1179	0.5232		7	5.6482	0.0908	0.5131
	8	4.7951	0.1110	0.5323		8	6.1774	0.0839	0.5181
	9	5.1191	0.1058	0.5418		9	6.6579	0.0786	0.5234
	10	5.4180	0.1018	0.5516		10	7.1000	0.0745	0.5288

Morlet	σ_t	σ_ω	Heis. Area
	0.7071	0.7071	0.5000

7 Examples

We now give some examples illustrating the usefulness of the wavelet tools.[11]

7.1 Example 1: The Wavelet Power

We have argued before that the main advantage of wavelet analysis over spectral analysis is the possibility of tracing transitional changes across time. To illustrate this, consider the following experiment with simulated data. We generate 50 years of monthly data according to the following data generating process:

$$y_t = \cos\left(\frac{2\pi}{p_1}t\right) + \cos\left(\frac{2\pi}{p_2}t\right) + \varepsilon_t, \quad t = \frac{1}{12}, \frac{2}{12}, \ldots, 50, \tag{64}$$

where $p_1 = 10$ and $p_2 = 5$, if $20 \leq t \leq 30$, and $p_2 = 3$, otherwise.

Formula (64) tells us that the time series y_t is the sum of two periodic components and a white noise.[12] The first periodic component represents a 10 year cycle, while the second periodic component shows some transient dynamics. In the beginning, it represents a 3 year cycle that, temporarily, changes to a 5 year cycle between the second and the third decades.

[11] For each example, there exists an associated script – named Example_*num*.m, where *num* is the example number – which can be used to generate all the pictures accompanying the example. These scripts are available in the folder Examples of the ASToolbox.

[12] This formulation is not as restrictive as it may seem. An autoregressive process of order 2, or higher, with an oscillatory behavior, will have a solution that involves sines and cosines. We, therefore, could have generated similar time series using a more common auto regressive process. We chose to explicitly have a cosine because the period of the oscillation is observed directly.

This change in the dynamics is nearly impossible to spot in Figure 3 (a). Furthermore, if we use the traditional spectral analysis, the information on the transient dynamics is completely lost, as we can see in Figure 3 (d). The power spectral density estimate is able to capture both the 3-year and the 10-year cycles but it completely fails to capture the 5-year cycle that occurred between the second and the third decades. Comparing with Figure 3 (c), we observe that spectral analysis gives us essentially the same information as the Global Wavelet Power Spectrum, which is an average, across time, of the Wavelet Power Spectrum.

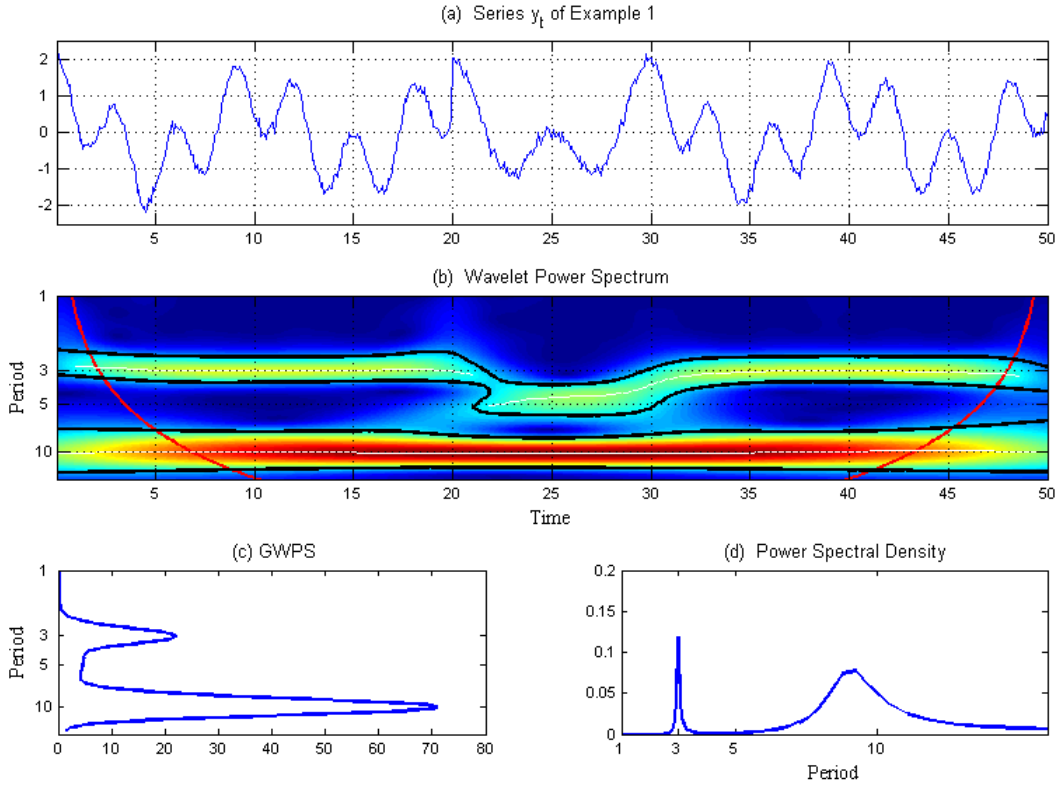

Figure 3: (a) $y_t = \cos(\frac{2\pi}{p_1}t) + \cos(\frac{2\pi}{p_2}t) + \varepsilon_t$. (b) Wavelet Power Spectrum of y_t - the thick black contour designates the 5% significance level based on an ARMA(1,1) null. The cone of influence, which indicates the region affected by edge effects, is shown with a red line. The color code for power ranges from blue (low Power) to red (high Power). The white lines show the maxima of the undulations of the Wavelet Power Spectrum. (c) Global Wavelet Power Spectrum - average Wavelet Power for each frequency. (d) Fourier Power Spectral Density.

On the other hand, Figure 3 (b) shows the Wavelet Power Spectrum itself. On the horizontal axis, we have the time dimension. The vertical axis gives us the periods. The

Power is given by the color. The color code for power ranges from blue (low Power) to red (high Power). Regions with warm colors represent areas of high Power. The white lines show the maxima of the undulations of the Wavelet Power Spectrum, therefore giving us a more precise estimate of the cycle period. The black contour designates the regions where the Wavelet Power is statistically significant at 5%. We observe a white line on period 10 across all times, meaning that there is a permanent cycle of this period. Both the red color and the black contour tell us that this cycle is strong and statistically significant. We are also able to spot the three year period cycle that occurs between time zero and 20 and, again, between time 30 and 50. Finally, we are also able to spot a yellow/orange region between time 20 and 30, with the white stripes identifying the cycle of period five. This means that a cycle of roughly 5-year periodicity, relatively important in explaining the total variance of the time-series and taking place between time 20 and 30, was hidden by the Fourier Power Spectrum estimate.

Figure 3 (b) clearly illustrates the big advantage of wavelet analysis over spectral analysis. While the Fourier transform is silent about changes that happen across time, with wavelets we are able to estimate the Power Spectrum as a function of time and, therefore, we do not loose the time dimension. The Wavelet Power Spectrum is able to capture not only the 3-year and 10-year cycles, but also to capture the change that occurred between years 20 and 30.

7.2 Example 2: The Great Moderation in the United Sates

In Figure 4 (a), we have the real GNP (quarterly) growth rate for the United States, from 1947q2 until 2010q1. In Figure 4 (b), one can observe the Wavelet Power Spectrum. At business cycle frequencies, the Wavelet Power was high and statistically significant, until early 1960s. After that, the volatility at all frequencies steadily decreased, with an exception between mid 1970s and 1984, when the variance at the business cycle frequency (1 to 8 years) was quite high again, probably as a result of the severe oil crisis that hit the world economy in 1973 and 1979 and lasted until the early 1980s.

The literature has identified 1984 as the year that marks the beginning of the Great Moderation (Kim and Nelson, [29]; McConnell and Pérez-Quirós, [33]). In reality, we can observe that this Great Moderation may have started sometime earlier. It was in the early 1960s that the volatility started to decrease. It then was revived, due to the oil shocks, at the business cycle frequency in the 1970s, however this increase was temporary. These results are in line with Blanchard and Simon [5] who have argued that the large shocks in the 1970s and the deep contraction in early 1980s hide from view the longer term volatility decline that began a few decades before. As one would expect, given the turbulence of the last years, after 2007 there is again evidence that volatility is increasing. We see this because the Wavelet Power Spectrum becomes statistically significant in the late 2000s at 1.5 to 5 years frequencies. Although part of this region may be affected by edge effects (because it is under the effect of the cone of influence), it is also true that because of the zero padding, this influence will tend to underestimate, instead of overestimate, the Power

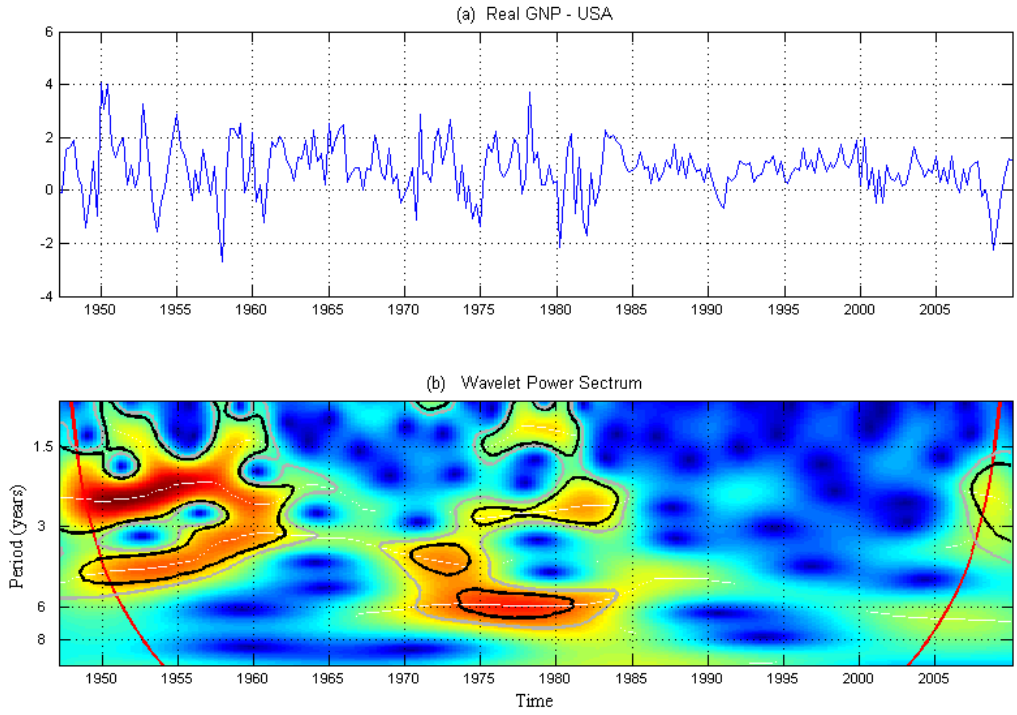

Figure 4: (a) GNP (quarterly) growth rate for the United States; (b) Wavelet Power Spectrum - the thick black contour designates the 5% significance level based on an ARMA(1,1) null and the grey contour the 10% significance level. The cone of influence, which indicates the region affected by edge effects, is shown with a red line. The color code for power ranges from blue (low Power) to red (high Power). The white lines show the maxima of the undulations of the Wavelet Power Spectrum.

Spectrum.

7.3 Example 3: The Cross-Wavelet and the Phase-Difference

Consider now two time series that share two common cycles, with some delays:

$$x_t = \sin\left(\frac{2\pi}{3}t\right) + 3\sin\left(\frac{2\pi}{6}t\right) + \varepsilon_{x,t}, \qquad t = 0, \frac{1}{12}, \frac{2}{12}, \ldots, 50, \tag{65}$$

$$y_t = \begin{cases} 4\sin\left(\frac{2\pi}{3}(t+\frac{4.5}{12})\right) - 3\sin\left(\frac{2\pi}{6}(t-\frac{9}{12})\right) + \varepsilon_{y,t}, & t = 0, \frac{1}{12}, \frac{2}{12}, \ldots, 25, \\ 4\sin\left(\frac{2\pi}{3}(t-\frac{4.5}{12})\right) - 3\sin\left(\frac{2\pi}{6}(t+\frac{9}{12})\right) + \varepsilon_{y,t}, & t = 25+\frac{1}{12}, 25+\frac{2}{12}, \ldots, 50; \end{cases} \tag{66}$$

see Figure 5 (a). Looking at the formulas, it is clear that x_t and y_t share 3-year and 6-year cycles. However, how their cycles relate to each other evolve with time and are different across frequencies from cycle to cycle. Consider the shorter period cycle, the 3-year cycle. The cycles are positively correlated. However, while for the first half of the sample the y_t cycle precedes the x_t cycle by 4 and a half months, in the second half of the sample the y_t cycle lags the x_t cycle.

These features are captured in Figure 5 (b)-(d). On the left, we have the Wavelet Coherency. On the right we have the Phases and Phase-Difference computed for two different frequency bands. On the top, we compute the phases for the $2.5 \sim 3.5$ year frequency band. In the bottom, we consider the $5 \sim 7$ year frequency band. The green line represents the y_t Phase and the blue represents the x_t Phase. The red line represents the Phase-Difference.

That both series have common and highly correlated 3-year and 6-year cycles is revealed by the regions of strong Coherency around those frequencies. That the 3-year cycles are in phase (positively correlated) is revealed by the Phase-Difference (red line in the upper right graph), which is consistently situated between $-\pi/2$ and $\pi/2$. Finally, we can see that the 3-year y_t cycle was leading for the first half of the time and lagging in the second half, by noting that in the first half of the sample the Phase-Difference is between zero and $\frac{\pi}{2}$, while in the second half it is between $-\frac{\pi}{2}$ and zero.

Looking at the 6-year cycle, we observe that the series are out of phase (negatively correlated) with x_t leading in the first half and y_t leading in the second half of the sample.

In this example, we observe that not only the wavelets are adequate to capture structural breaks and transient relations, but that they can also distinguish between different relations that occur at the same time but at distinct frequencies.

7.4 Example 4: Business Cycle Synchronization Between Portugal and Spain

In Figure 6 (a), we have the industrial production (yearly) growth rates for Portugal (blue line) and Spain (green line), from 1970:01 until 2010:05. We can use Wavelet Coherency, the Phases, and Time-Lag, to check how synchronized the business cycle is between these

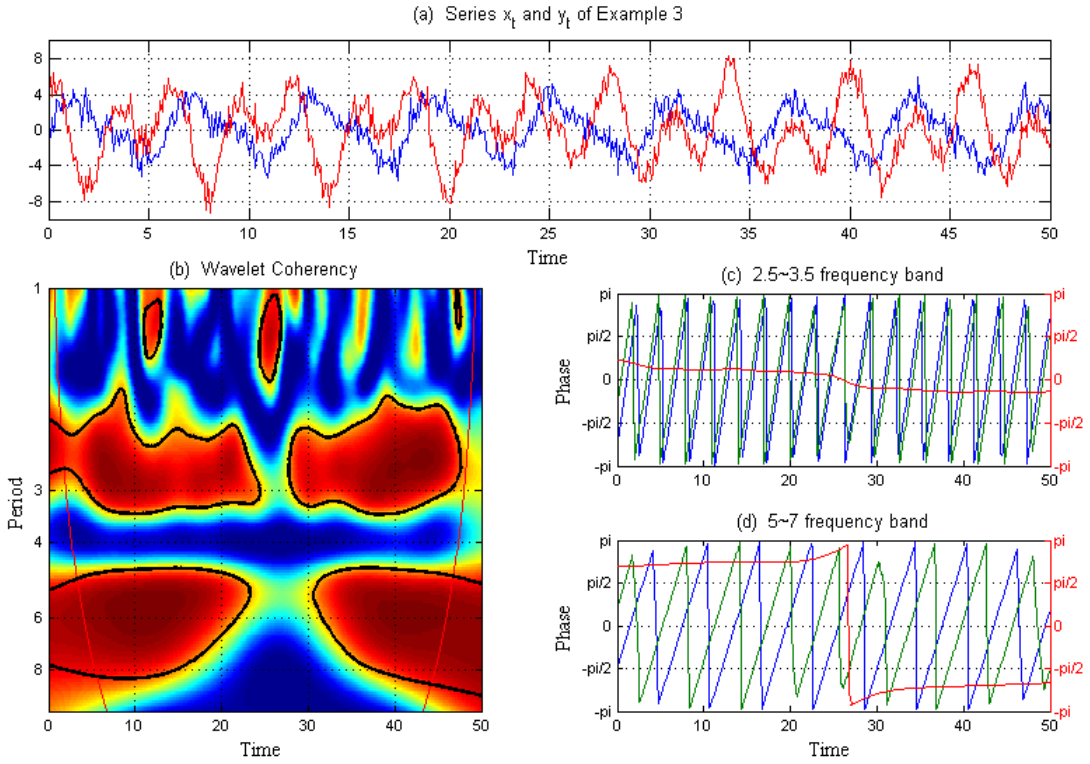

Figure 5: (a) x_t (blue line) given by Eq.(65) and y_t (red line) given by Eq.(66). (b) Wavelet Coherency - the cone of influence is shown with a red line. The thick contour designates the 5% level based on a ARMA(1,1) null. Coherency ranges form blue (low Coherency) to red (high Coherency). (c) - (d) Phases and Phase-Difference. The green line represents the y_t Phase, the blue line the x_t Phase and the red line represents the Phase-Difference; (c) is for the $2.5 \sim 3.5$ year frequency band and (d) for the $5 \sim 7$ year frequency band.

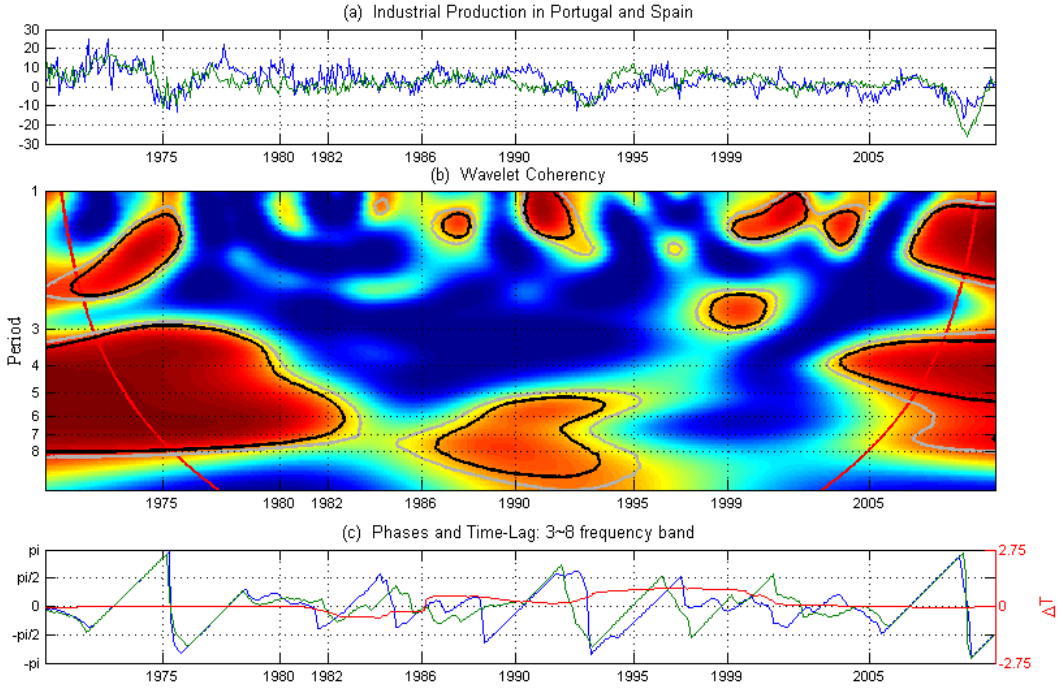

Figure 6: (a) Industrial production (yearly) growth rates for Portugal (blue line) and Spain (green line). (b) Wavelet Coherency - the cone of influence is shown with a red line. The black thick contour designates the 5% significance level based on an ARMA(1,1) null and the grey contour the 10% significance level. Coherency ranges form blue (low Coherency) to red (high Coherency). (c) Phases and Time-Lag - The blue line represents the Phase for Portugal, the green line the Phase for Spain and the red line represents the Instantaneous Time-Lag between Spain and Portugal.

two countries. In 6 (b), we see that until early 1980s, the two time series are highly coherent and in 6 (c) we observe that their Phases, at business cycle frequencies $3 \sim 8$ years period cycles, were almost perfectly aligned in this period. Although the precise details are different, these two countries, in the first half of the decade of 1970, had proto-fascist regimes (Kallis [28]) and in the second half of the decade they became democratic. They applied together to be part of the European Economic Community, which they joined in the first of January of 1986. In 1982, Portugal had a severe Current Account crisis that led to an IMF intervention in 1983. This coincides with the de-synchronization between the two countries business cycles. Between 1986 and 1995, the two countries became more synchronized again, as we can see in 6 (b), however the Phases were not aligned anymore. Instead, the Time-Lag betwwen Spain and Portugal (red line) tells us that the Portuguese business cycle was lagging the Spanish one. After 1999, when both countries joined the Euro, the Time-Lag started approaching zero. After 2002, the Time-Lag became almost zero, suggesting that the business cycles became aligned again. After 2004, we also observe a region of high Coherency, which reinforces our previous conclusion. Therefore, coinciding with the adoption of a common currency, the business cycles became more synchronized.

7.5 Example 5: Frequency versus Time Accuracy

The purpose of this example is to illustrate the influence of the wavelet on the results of the corresponding AWT.

We first consider a series which is a sum of two pure oscillations, corrupted with some noise:

$$x_t = \cos(2\pi t/3) + \cos(2\pi t/4.5) + \varepsilon_t; \quad t = \frac{1}{12}, \frac{2}{12}, \ldots, 50; \tag{67}$$

see Fig 7 (a). The first periodic component corresponds to a 3 year cycle and the second to a 5 year cycle. We analyze this series with three different wavelets: two GMWs $\psi_{\beta,\gamma}$, the first with $\beta = 8$ and $\gamma = 10$ and the second with $\beta = 20$ and $\gamma = 0.5$, and the Morlet Wavelet ψ_ω^M with $\omega = 6.0$. The values of the time-radius, frequency-radius and Heisenberg area of these wavelets are given by

$$\begin{array}{lll} \sigma_{t;8,10} = 6.5034 & \sigma_{\omega;8,10} = 0.0823 & A_{\psi_{8,10}} = 0.5352 \\ \sigma_{t;20,0.5} = 0.0014 & \sigma_{\omega;20,0.5} = 376.9287 & A_{\psi_{20,0.5}} = 0.54015 \\ \sigma_{t;\psi^M_{6.0}} = 0.7071 & \sigma_{\omega;\psi^M_{6.0}} = 0.7071 & A_{\psi^M_{6.0}} = 0.5 \end{array} \tag{68}$$

Hence, the wavelet with best localization in frequency is the GMW $\psi_{8,10}$, whilst the one with worst localization in frequency is $\psi_{20,0.5}$. The Morlet Wavelet has a frequency localization between the other two wavelets. Figure 7 (b) displays the wavelet power computed with each of these wavelets. Observing this picture, the different capacities of frequency localization of the wavelets becomes very apparent. On the left, we have the Power computed with the GMW $\psi_{8,10}$ and we are able to fully separate the 3 year cycle, from the 4.5 year cycle. The picture in the middle corresponds to the use of the wavelet with the poorest frequency

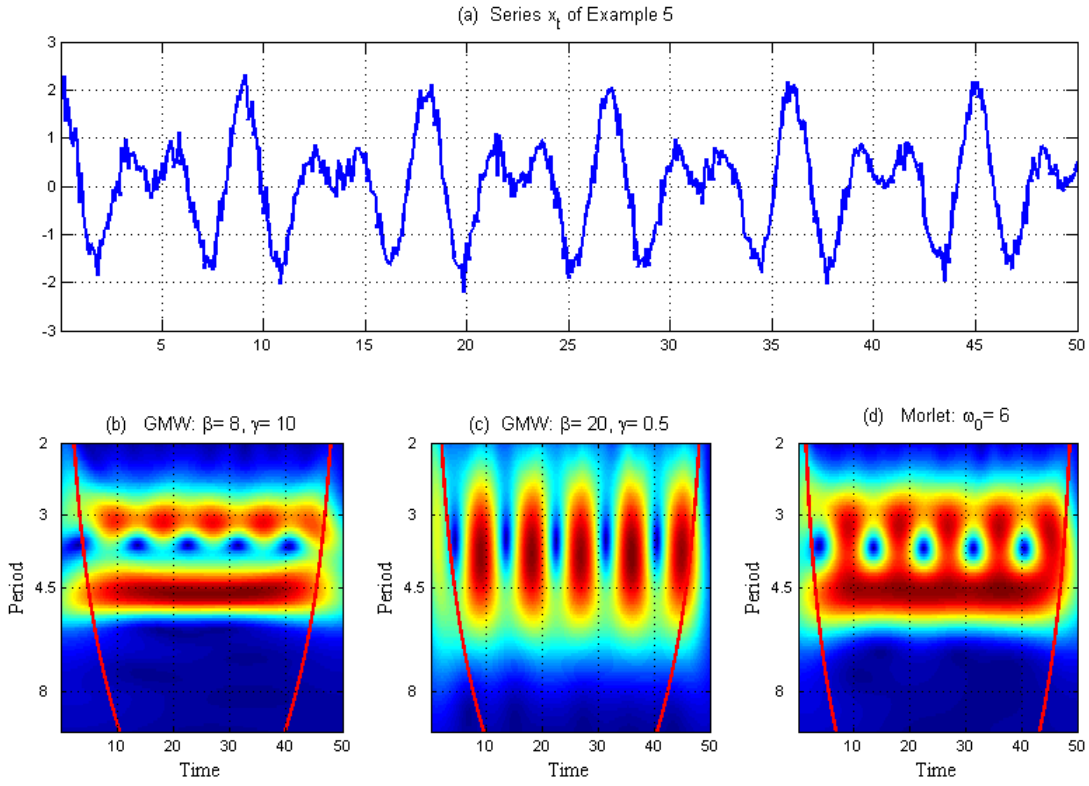

Figure 7: (a) $x_t = \cos(2\pi t/3) + \cos(2\pi t/4.5) + \varepsilon_t$. (b) - (d) Wavelet Power Spectrum of x_t using: (b) GMW $\psi_{8,10}$; (c) GMW $\psi_{20,0.5}$; (d) Morlet with $\omega_0 = 6.0$

localization, the GMW $\psi_{20,0.5}$. With this wavelet, we completely loose the capacity to discriminate the two periods. Finally, with the Morlet Wavelet, whose picture is on the right, we can still recognize the two periodic components, although not so clearly.

To test the different capacities of localization in time, we consider the case of a series y_t corresponding to the sum of two Dirac-delta functions:

$$y_t = \begin{cases} 0 & \text{for } t = \frac{1}{12}, \frac{2}{12} \ldots, 50, \ t \neq 20, 30, \\ 1 & \text{for } t = 20, 30. \end{cases} \tag{69}$$

We again analyze this series with the same three wavelets considered before. As far as localization in time is concerned, we observe that the wavelet $\psi_{10,0.25}$ is the best localized, followed by the Morlet, the GMW $\psi_{8,10}$ being the worst of all.

In Figure 8, which displays the Wavelet Power computed with each of these wavelets, one can clearly distinguish the time discrimination capacities of the wavelets.

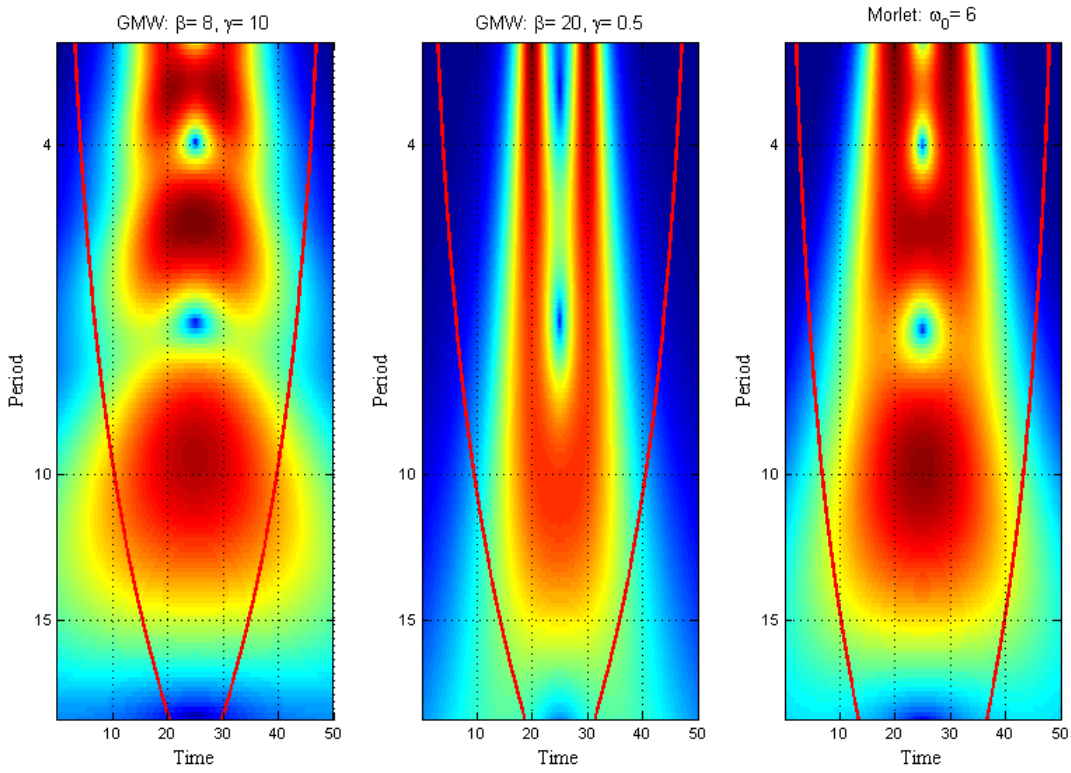

Figure 8: Wavelet Power Spectrum of y_t of Eq.(69) using: (a) GMW $\psi_{8,10}$; (b) GMW $\psi_{20,0.5}$; (c) Morlet with $\omega_0 = 6.0$

8 Conclusion

In this paper, we argued that Wavelet Analysis can be a very useful tool to analyze business cycles. The main objective of this paper was to present a self-contained summary on the most relevant theoretical results related to the Continuous Wavelet Transform and to describe how such transforms can be implemented in practice. We also presented some results on a new family of wavelets, the Generalized Morse Wavelets, which are becoming more popular in other scientific fields and allow for more flexibility than the popular Morlet Wavelet, while keeping some of its nice properties. To illustrate the potentialities of Wavelet Analysis and to provide some easy to do examples, we worked out four constructed examples and two real data applications. The constructed examples were put together to show how Wavelet Analysis can easily capture transient cycles that are not stable across time and frequencies; how cross wavelets can capture transient relationships between two time-series at different frequencies; and to illustrate different mother wavelets perform in the time-frequency domains with different types of signals. We also provide two applications with real data. In one of them, we study the post-war business cycle volatility in the United States, by looking at real GNP growth rates. We concluded that while it is true that business cycles were very active during the 70s and early 80s (after the oil price shocks in the 70s), it is also true that our results support the view of Blanchard and Simon [5], according to whom the large shocks in the 1970s disguised the fact that the moderation had begun a few decades earlier. We also used Industrial Production data for Portugal and Spain since 1970 to analyze the synchronization between their business cycles. Who showed that while both countries had authoritarian proto-fascist regimes, their business cycles were highly coordinated, and that after 1986, when both countries joined the European Union, Portuguese cycles lagged the Spanish ones, until both countries adopted a common currency in 1999. After that point in time, their cycles became more coordinated and, by 2004 their cycles were, again, perfectly aligned.

Attached to this paper, there is a Matlab toolbox implementing the referred wavelet tools, which the researcher can freely use and adapt to his/her own research.

References

[1] L. Aguiar-Conraria, N. Azevedo, and M. J. Soares. Using wavelets to decompose the time-frequency effects of monetary policy. *Physica A: Statistical Mechanics and its Applications*, 387(12):2863–2878, 2008.

[2] L. Aguiar-Conraria and M. J. Soares. Oil and the macroeconomy: using wavelets to analyze old issues. *Journal Empirical Economics*, (forthcoming).

[3] P. Baubeau and B. Cazelles. French economic cycles: a wavelet analysis of French retrospective GNP series. *Cliometrica*, 3(3):275–300, 2009.

[4] J. Berkowitz and L. Kilian. Recent developments in bootstrapping time series. *Econometric Reviews*, 19(1):1–48, 2000.

[5] O. Blanchard and J. Simon. The long and large decline in U.S. output volatility. *Brookings Papers on Economic Activity*, 1:135–164, 2001.

[6] P. Brémaud. *Mathematical Principles of Signal Processing: Fourier and Wavelet Analysis*. Springer-Verlag, 2002.

[7] B. Cazelles, M. Chavez, G. C. de Magny, J.-F. Guégan, and S. Hales. Time-dependent spectral analyisis of epidemiological time-series with wavelets. *Journal of the Royal Society Interface*, 4:625–636, 2007.

[8] S. Chatterjee. Bootstrapping ARMA models: Some simulations. *IEEE Transactions on Systems, Man and Cybernetics*, SMC-16(2):294–299, 1986.

[9] J. Connor and R. Rossiter. Wavelet transforms and commodity prices. *Studies in Nonlinear Dynamics and Econometrics*, 9(1):Article 6, 2005.

[10] P. Crowley and D. Mayes. How fused is the Euro area core? : An eavaluation of growth cycle co-movement and synchronization using wavelet analysis. *J. Bus. Cycle. Meas. Anal.*, 4:63–95, 2008.

[11] P. M. Crowley. A guide to wavelets for economists. *Journal of Economic Surveys*, 21:207–267, 2007.

[12] I. Daubechies. *Ten Lectures on Wavelets*, volume 61 of *CBMS-NSF Regional Conference Series in Applied Mathematics*. SIAM, Philadelphia, 1992.

[13] N. Delprat, B. Escudié, P. Guillemain, R. Kronland-Martinet, P. Tchamitchian, and B. Torrésani. Asymptotic wavelet and Gabor analysis: Extraction of instantaneous frequencies. *IEEE Trans. Inf. Theory,*, 38(2):644–665, 1992.

[14] M. Farge. Wavelet transforms and their applications to turbulence. *Annu. Rev. Fluid Mech.*, 24:395–457, 1992.

[15] V. Fernandez. The international CAPM and a wavelet-based decomposition of value at risk. *Studies in Nonlinear Dynamics and Econometrics*, 9(4):Article 4, 2005.

[16] E. Foufoula-Georgiou and P. Kumar. Wavelets in geophysics. In *Wavelet Analysis and Its Applications*, volume 4. Academic Press, 1994.

[17] M. Gallegati and M. Gallegati. Wavelet variance analysis of output in G-7 countries. *Studies in Nonlinear Dynamics and Econometrics*, 11(3):Article 6, 2007.

[18] Z. Ge. Significance testst for the wavelet power and the wavelet power spectrum. *Ann. Geophys.*, 25:2259–2269, 2007.

[19] Z. Ge. Significance tests for the wavelet cross spectrum and wavelet linear coherence. *Ann. Geophys.*, 26:3819–3829, 2008.

[20] R. Gençay, F. Selçuk, and B.Withcher. Differentiating intraday seasonalities through wavelet multi-scaling. *Physica A: Statistical Mechanics and its Applications*, 289(3-4):543–556, 2001.

[21] R. Gençay, F. Selçuk, and B.Withcher. Scaling properties of foreign exchange volatility. *Physica A: Statistical Mechanics and its Applications*, 289(1-2):249–266, 2001.

[22] R. Gençay, F. Selçuk, and B.Withcher. Multiscale systematic risk. *Journal of International Money and Finance*, 24:55–70, 2005.

[23] P. Goupillaud, A. Grossman, and J. Morlet. Cycle-octave and related transforms in seismic signal analysis. *Geoexploration*, (23):85–102, 1984.

[24] A. Grinsted, J. C. Moore, and S. Jevrejeva. Application of the cross wavelet transform and wavelet coherence to geophysical time series. *Nonlinear Proc. Geoph.*, 11:561–566, November 2004. Part of Special Issue Nonlinear analysis of multivariate geoscientific data- advanced methods, theory and application.

[25] M. Holschneider. *Wavelets: An Analysis Tool*. Clarendon Press, Oxford, 1995.

[26] L. Hudgins, C. A. Friehe, and M. E. Mayer. Wavelet transforms and atmospheric turbulence. *Phys.Rev. Lett.*, 71(20):3279–3282, 1993.

[27] T. Jagrič and R. Ovin. Method of analyzing business cycles in a transition economy: The case of Slovenia. *The Developing Economies*, 42(1):42–62, 2004.

[28] A. A. Kallis. The 'regime-model' of Fascism: A typology. *European History Quarterly*, 30(1):77–104, 2000.

[29] C.-J. Kim and C. Nelson. Has the U.S. Economy become more stable? a Bayesian approach based on a Markov-switching model of the business cycle. *Review of Economics and Statistics*, 81:608–616, 1999.

[30] J. M. Lilly and S. C. Olhede. On the analytic wavelet transform. *IEEE Transactions on Signal Processing*, 1(11):1–15, 2007.

[31] J. M. Lilly and S. C. Olhede. Higher-order properties of analytic wavelets. *IEEE T. Signal Proces.*, 57(1):146–160, 2009.

[32] S. Mallat. *A Wavelet Tour of Signal Processing*. Academic Press, New York, 1998.

[33] M. McConnel and G. Pérez-Quirós. Output fluctuations in the United States: What has changed since the early 1980s? *American Economic Review*, 90:1464–1476, 2000.

[34] S. C. Olhede and A. T. Walden. Generalized Morse wavelets. *IEEE T. Signal Proces.*, 50(11):2661–2670, 2002.

[35] S. M. Raihan, Y. Wen, and B. Zeng. Wavelet: A new tool for business cycle analysis. Working Paper 2005-050A, Federal Reserve Bank of St. Louis, 2005.

[36] J. B. Ramsey. The contribution of wavelets to the analysis of economic and financial data. *Philosophical Transactions of the Royal Society of London Series A*, 357:2593–2606, 1999.

[37] J. B. Ramsey. Wavelets in economics and finance: past and future. *Studies in Nolinear Dynamics and Econometrics*, 6(3):Article1, 2002.

[38] J. B. Ramsey and C. Lampart. The decomposition of economic relationships by timescale using wavelets: Expenditure and income. *Studies in Nonlinear Dynamics and Econometrics*, 3(4):23–42, 1998.

[39] J. B. Ramsey and C. Lampart. Decomposition of economic relationships by timescale using wavelets: Money and income. *Macroeconomics Dynamics*, 2:49–71, 1998.

[40] A. Rua. Measuring comovement in the time-frequency space. *Journal of Macroeconomics*, 32:685–691, 2010.

[41] A. Rua and L. C. Nunes. International comovement of stock market returns: A wavelet analysis. *Journal of Empirical Finance*, 16(4):632–639, 2009.

[42] I. W. Selesnick, R. G. Baraniuk, and N. G. Kinsbury. The dual-tree complex wavelet transform. *IEEE Signal Process. Mag.*, 22:123–151, 2005.

[43] C. Torrence and G. P. Compo. A practical guide to wavelet analysis. *Bull. Am. Meteorol. Soc.*, 79:61–78, 1998.

[44] C.-L. Tu, W.-L. Hwang, and J. Ho. Analysis of singularities from modulus maxima of complex wavelets. *IEEE Trans. Inf. Theory*, 51:10491062, 2005.

[45] H. Wong, W.-C. Ip, Z. Xie, and X. Lui. Modelling and forecasting by wavelets, and the application to exchange rates. *Journal of Applied Statistics*, 30(5):537553, 2003.

A ASToolbox

The folder ASToolbox contains a series of matlab functions implementing the continuous wavelet tools described in this paper. Our main objective was to collect into one single directory all the functions necessary to use these tools and also to provide some scripts illustrating their use. This, we hope, will encourage newcomers to the field to make tests with their own data and might contribute to the dissemination of the use of wavelets, not only in economics and finance, but possibly in other areas.

Please acknowledge the use of our functions in any publications:
Wavelet software was provided by L. Aguiar-Conraria and M. J. Soares and is available at http://sites.google.com/site/aguiarconraria/joanasoares-wavelets We would also appreciate that a copy of such publications was sent to one of us.
Any critics, comments and suggestions to improve our functions are most welcome!

The folder **ASToolbox** is divided into two sub-folders:

1. **Functions** – containing all the matlab functions. This has two sub-folders:
   - **Auxiliary** – containing some auxiliary functions to, e.g. generate surrogate series or compute Fourier spectra; it also contains a function to compute measures associated with generalized Morse wavelets.
   - **WaveletTransforms** – containing functions to compute the (Analytic) Wavelet Transform, Cross-Wavelet Transform, Wavelet Coherency, Wavelet Phase-Difference and Time-Lag.
2. **Examples** – containing matlab scripts to generate the pictures associated with each of the Examples in Section 7.

Some of our functions are based on (parts of) functions written by Christopher Torrence and Gilbert P. Compo (http://paos.colorado.edu/research/wavelets/) and also on some modified versions of functions written by Bernard Cazelles and Mario Chavez; [7].

Apart from some computational choices and the correction of some typos, there are three main differences: (1) the capacity of using an entire family of analyzing wavelets, the GMWs, (2) the possibility of changing the wavelet parameters, allowing for greater flexibility, and (3) different null hypothesis for testing significance.

A.1 Implementation details

When implementing the transforms, some choices have, naturally, to be made. We now give a brief description of the options made in our programs. These can be modified, with very little effort, by any user.

- **Normalization**

  The wavelets are normalized to have unit energy, i.e. we use formula (57) for the normalizing constant, in the case of a GMW $\psi_{\beta;\gamma}$, and formula (51), in the case of the Morlet Wavelet.

- **Fourier factor**

  The conversion of scales to frequencies is based on the energy frequency ω_ψ^E, given by (29), i.e. we use formula $\omega(s) = \frac{\omega_\psi^E}{s}$ to convert scales to angular frequencies. This, in turn, means that our Fourier factor, used to convert scales to Fourier periods, is given by

  $$\mathrm{Ff} = \frac{s}{\omega_\psi^E}. \tag{70}$$

- **Formula for CWT**

  The implementation of the CWT (and, hence, also the XWT and the WCO) is based on the use of formula (46), together with and inverse FFT.

- **Scales**

  The scales used in the CWT (XWT, WCO) are chosen as fractional powers of 2, i.e. they are of the type given by (47).

- **COI**

  When implementing our algorithms, we take as decaying time to define the COI, the quantity given by the radius of the wavelet (at each scale s_ℓ), i.e. we consider

  $$t_\ell = s_\ell \sigma_t,$$

  where σ_t is given by formula (19). But

  $$t_\ell = s_\ell \sigma_t \iff t_\ell = \frac{\lambda_\ell}{\mathrm{Ff}} \sigma_t \iff \lambda_\ell = \frac{\mathrm{Ff}}{\sigma_t} t_\ell, \tag{71}$$

  where λ_ℓ denotes the Fourier period corresponding to scale s_ℓ and Ff is the Fourier factor given by (70).

- **Smoothing**

  The smoothing process involved in the coherency computations is done by convolution with window functions in time and in frequency. The type and size of the window can be selected by the user. Possible windows are: rectangular (box), triangular, Hamming, Hanning, Blackman and Bartlett.

- **Significance tests**

  The tests of significance are always based on Monte Carlo simulations. The simulations use two different types of methods to construct surrogate series: (1) fitting an ARMA(p, q) model and building new samples by bootstrap or (2) fitting an ARMA(p, q) model and construct new samples by drawing errors from a Gaussian distribution. In the first option, we use the very basic bootstrap technique described in Section 2.1 of Berkowitz and Kilian [4] and Chatterjee [8]. In the second option, the surrogates are constructed using the function 'garchsim' (univariate GARCH process simulation) of the Econometrics Toolbox included in MatLab 2009. To fit the ARMA(p, q) to the data, we make use of the function 'garchfit' of the same toolbox. The user that does not have the Econometrics toolbox can perform significance tests by choosing an ARMA$(p, 0)$ model with bootstrap. In this case, the AR(p) model is estimated by OLS and the code is self-contained and autonomous from the Econometrics toolbox.

A.2 Software requirements

Our programs were written in Matlab 2009.b. However we were careful in writing it in such a way that it is fully compatible with version 7. Some of our programs make use of functions from the Matlab toolboxes Econometrics Toolbox, Signal Processing Toolbox and Statistics Toolbox. This is always explicitly stated in the function and may, in some cases, be very simply replaced by functions written by the user.

A.3 List of functions

The following functions are available.

1. Folder **Auxiliary**
   - AROLS - AR model of a time series based on Ordinary Least Squares.
   - FourierSpectrum - Parametric estimate of the Fourier Power Spectrum of a time series, by fitting an ARMA process.
   - GMWMeasures - Some measures associated with a given Generalized Morse Wavelet.
   - MatrixMax - Local maxima of a matrix.
   - ProcessMatrix - Pre-processing of columns of given matrix.
   - SurrogateARMABoot - Surrogate series based on ARMA model and bootstrap.
   - SurrogateARMAEcon - Surrogate series using Econometrics toolbox.
   - WaveletSpectra - Wavelet transforms of all the columns of a given matrix.
2. Folder **WaveletTransforms**
   - AWCO - Wavelet Coherency and Cross Wavelet Transform of two series.

- AWCOOutput - Different quantities computed from a Wavelet Coherency.
- AWT - Analytic Wavelet Transform of given series.
- AWTOutput - Different quantities computed from a Wavelet Transform.

Most Recent Working Paper

NIPE WP 23/2010	**Aguiar-Conraria e Maria Joana Soares,** "The Continuous Wavelet Transform: A Primer*", 2010
NIPE WP 22/2010	**Alexandre, Fernando, Pedro Bação, João Cerejeira e Miguel Portela,** "Manufacturing employment and exchange rates in the Portuguese economy: the role of openness, technology and labour market rigidity", 2010
NIPE WP 21/2010	**Aguiar-Conraria, Luís, Manuel M. F. Martins e Maria Joana Soares,** "The yield curve and the macro-economy across time and frequencies", 2010
NIPE WP 20/2010	**Kurt Richard Brekke, Tor Helge Holmås e Odd Rune Straume,** "Margins and Market Shares: Pharmacy Incentives for Generic Substitution", 2010
NIPE WP 19/2010	**Afonso, Óscar, Pedro Neves e Maria Thopmson,** "Costly Investment, Complementarities, International Technological-Knowledge Diffusion and the Skill Premium", 2010
NIPE WP 18/2010	**Mourão, Paulo e Linda G. Veiga,** "Elections, Fiscal Policy and Fiscal Illusion", 2010
NIPE WP 17/2010	**Conraria, Luís A., Pedro C. Magalhães, Maria Joana Soares,** "Synchronism in Electoral Cycles: How United are the United States? ", 2010
NIPE WP 16/2010	**Figueiredo, Adelaide, Fernanda Figueiredo, Natália Monteiro e Odd Rune Straume,** "Restructuring in privatised firms: a Statis approach", 2010
NIPE WP 15/2010	**Sousa, Ricardo M.,** "Collateralizable Wealth, Asset Returns, and Systemic Risk: International Evidence", 2010
NIPE WP 14/2010	**Sousa, Ricardo M.,** "How do Consumption and Asset Returns React to Wealth Shocks? Evidence from the U.S. and the U.K", 2010
NIPE WP 13/2010	**Monteiro, Natália., Miguel Portela e Odd Rune Straume,** "Firm ownership and rent sharing", 2010
NIPE WP 12/2010	**Afonso, Oscar, Sara Monteiro e Maria Thompson.,** "A Growth Model for the Quadruple Helix Innovation Theory ", 2010
NIPE WP 11/2010	**Veiga, Linda G.,**" Determinants of the assignment of E.U. funds to Portuguese municipalities", 2010
NIPE WP 10/2010	**Sousa, Ricardo M.,** "Time-Varying Expected Returns: Evidence from the U.S. and the U.K", 2010
NIPE WP 9/2010	**Sousa, Ricardo M.,** "The consumption-wealth ratio and asset returns: The Euro Area, the UK and the US", 2010
NIPE WP 8/2010	**Bastos, Paulo, e Odd Rune Straume,** "Globalization, product differentiation and wage inequality", 2010
NIPE WP 7/2010	**Veiga, Linda, e Francisco José Veiga,** "Intergovernmental fiscal transfers as pork barrel", 2010
NIPE WP 6/2010	**Rui Nuno Baleiras,** "Que mudanças na Política de Coesão para o horizonte 2020?", 2010
NIPE WP 5/2010	**Aisen, Ari, e Francisco José Veiga,** "How does political instability affect economic growth?", 2010
NIPE WP 4/2010	**Sá, Carla, Diana Amado Tavares, Elsa Justino, Alberto Amaral,** "Higher education (related) choices in Portugal: joint decisions on institution type and leaving home", 2010
NIPE WP 3/2010	**Esteves, Rosa-Branca,** "Price Discrimination with Private and Imperfect Information ", 2010
NIPE WP 2/2010	**Alexandre, Fernando, Pedro Bação, João Cerejeira e Miguel Portela,** "Employment, exchange rates and labour market rigidity", 2010
NIPE WP 1/2010	**Aguiar-Conraria, Luís, Pedro C. Magalhães e Maria Joana Soares,** "On Waves in War and Elections - Wavelet Analysis of Political Time-Series", 2010
NIPE WP 27/2009	**Mallick, Sushanta K. e Ricardo M. Sousa,** "Monetary Policy and Economic Activity in the BRICS", 2009
NIPE WP 26/2009	**Sousa, Ricardo M.,** " What Are The Wealth Effects Of Monetary Policy?", 2009
NIPE WP 25/2009	**Afonso, António., Peter Claeys e Ricardo M. Sousa,** "Fiscal Regime Shifts in Portugal", 2009